Chapter 2
Flight Dynamic Models

2.1 Aims and Objectives

- To present the basic flight dynamics modeling approach applicable to aircraft, rockets, and spacecraft
- To derive the equations of motion for typical flight dynamic systems
- To describe the sensors used in flight control systems

2.2 Rigid Body Dynamics

The word "dynamics" refers to the motion of a body, which can be completely described by velocity (kinematics) and acceleration (kinetics). Kinematical equations of translation and rotation are derived using the geometry of motion. When Newton's laws are applied, we obtain kinetic equations for both translation and rotation. Considering the vehicle as a body (collection of a large number of particles) of mass m acted upon by external force $\mathbf{F}(t)$, we apply Newton's second law of motion relative to an *inertial frame* of reference $(o_G x_G y_G z_G)$ (Fig. 2.1) to individual particles of mass δm and take a sum over all particles:

$$\sum \delta \mathbf{F} = \frac{\mathrm{d}}{\mathrm{d}t} \sum \mathbf{v} \delta m. \tag{2.1}$$

Due to Newton's third law of motion, the internal forces acting between any two particles cancel out. Consequently, the net force on the body is the same as the external force $\mathbf{F}(t)$. Furthermore, the instantaneous velocity of a point o attached to the body is given as $\mathbf{v} = \frac{\mathrm{d}(\mathbf{r})}{\mathrm{d}t}$, where $\mathbf{r}(t)$ is the instantaneous position of o. There is a special point associated with every body, called the *center of mass*, such that the

A. Tewari, *Automatic Control of Atmospheric and Space Flight Vehicles: Design and Analysis with MATLAB® and Simulink®*, Control Engineering,
DOI 10.1007/978-0-8176-4864-0_2, © Springer Science+Business Media, LLC 2011

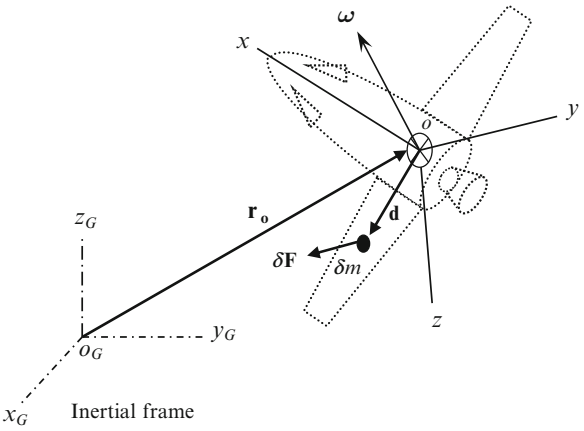

Fig. 2.1 Rotation and translation of a flight vehicle

mass moment, $\sum \mathbf{d}\delta m$ vanishes about that point (Fig. 2.1). If we choose the point o to be the center of mass, then the governing translational kinetics equation, (2.1), can be written as follows:

$$\mathbf{F} = m\frac{\mathrm{d}\mathbf{v}}{\mathrm{d}t}. \tag{2.2}$$

A generic flight vehicle's mass m changes with time, either due to burning and ejection of a propellant mass, or addition/subtraction of modules (e.g., expenditure of munitions, docking of two spacecraft, etc.). Aerospace vehicles powered by rocket engines and those involving addition/subtraction of modules have a large instantaneous rate of change of mass, thereby generating a reactive force. For all other flight vehicles, the instantaneous rate of change of mass is relatively small and the vehicle's mass can be assumed constant over short portions of flight. When applying (2.2) to a variable mass vehicle, it must be ensured that the external force $\mathbf{F}$ includes all reactive forces due to mass ejection/accretion. It is clear from (2.2) that for the limited purpose of studying the translational motion of a body, we can regard the body as if all its mass were concentrated at the center of mass, and the net external force were applied at the center of mass. This forms the basis for the idealization of the body as a particle.

In flight control applications, it is more useful to resolve the force $\mathbf{F}$ and the velocity $\mathbf{v}$ in a *body-fixed* frame ($oxyz$) – a coordinate frame rigidly fixed to the body (Fig. 2.1) – rather than the inertial frame ($o_G x_G y_G z_G$). In that case, (2.2) becomes

$$\mathbf{F} = m\frac{\partial \mathbf{v}}{\partial t} + m(\boldsymbol{\omega} \times \mathbf{v}), \tag{2.3}$$

where the partial derivative denotes time derivative relative to the body-fixed frame and $\boldsymbol{\omega}$ is the *angular velocity* of the body (same as the angular velocity of the frame

($oxyz$)). For convenience of notation, we shall replace the partial time derivative with an overdot and write (2.3) as follows:[1]

$$\mathbf{F} = m\dot{\mathbf{v}} + m(\boldsymbol{\omega} \times \mathbf{v}). \tag{2.4}$$

The angular velocity is not a free variable, but must satisfy the governing equation of *rotational kinetics* obtained by taking moments of (2.1) about the center of mass, o:

$$\boldsymbol{\tau} = \sum \left(\mathbf{d} \times \delta m \frac{\mathrm{d}\mathbf{v}}{\mathrm{d}t} \right) = \int \left(\mathbf{d} \times \frac{\mathrm{d}\mathbf{v}}{\mathrm{d}t} \right) \mathrm{d}m, \tag{2.5}$$

where $\mathbf{d}$ is the position of the elemental mass δm relative to o (Fig. 2.1), $\bar{\mathbf{v}} = \mathbf{v} + \boldsymbol{\omega} \times \mathbf{d}$ the velocity of the elemental mass, and $\boldsymbol{\tau} \doteq \sum(\mathbf{d} \times \delta\mathbf{F})$ is the net *external torque* about o. Note that (2.5) involves a replacement of the summation over particles by an integration over mass in the limit $\delta m \to 0$, and also implies mutual cancellation of the internal torques. As in the case of translational dynamics, we require that $\boldsymbol{\tau}$ includes all reactive torques arising because of mass ejection/accretion from the vehicle. Equation (2.5) arises due to the fact that all the external forces may not pass through the center of mass, o, and constitutes a departure from particle idealization. Equation (2.5) can be rewritten in terms of the *angular momentum*, which is defined for the elemental mass by $\delta\mathbf{H} \doteq \mathbf{d} \times \delta m \bar{\mathbf{v}}$, and for the body by the following equation:

$$\mathbf{H} = \int \mathbf{d} \times \bar{\mathbf{v}} \mathrm{d}m. \tag{2.6}$$

If we assume the flight vehicle to be a *rigid body*,[2] we have

$$\mathbf{H} = \int \mathbf{d} \times (\boldsymbol{\omega} \times \mathbf{d}) \mathrm{d}m. \tag{2.7}$$

Substitution of (2.7) into (2.5) yields the following equation governing the rotational kinetics:

$$\frac{\mathrm{d}\mathbf{H}}{\mathrm{d}t} = \boldsymbol{\tau}. \tag{2.8}$$

The inherent coupling of rotational and translational kinetics is evident in (2.2) and (2.8), where $\boldsymbol{\omega}$ is common to both, and is obtained from the solution to the rotational kinetics equation, (2.8). Furthermore – as in all atmospheric flight vehicles and some spacecraft – if the external force vector depends on the vehicle's attitude (rotational variables), and the external torque vector depends upon position and velocity (translational variables), then a further coupling takes place between the rotation and the translation. When the time scale of rotation is much smaller

[1] The time derivative relative to a rotating frame is given by the chain rule $\dot{\mathbf{A}} = \frac{\partial \mathbf{A}}{\partial t} = \frac{\mathrm{d}\mathbf{A}}{\mathrm{d}t} - (\boldsymbol{\omega} \times \mathbf{A})$.

[2] The distance between any two points in a rigid body does not vary with time.

than that of translation (as in most spacecraft), then the two can be effectively decoupled. In such a case, the instantaneous rotational parameters are treated as inputs to the translatory motion, and the position and velocity are treated as almost constant parameters for the rotary motion. However, the decoupling of rotational and translational motions is not a good approximation either for a high performance aircraft or a missile, which would require a simultaneous solution of the two sets of equations ((2.2) and (2.8)), along with the kinematical equations discussed later.

In order to derive an expression for the angular momentum for use in the rotational kinetics equation (2.8), we resolve all the vectors in the body-fixed frame ($oxyz$) as follows:

$$\mathbf{d} = x\mathbf{i} + y\mathbf{j} + z\mathbf{k} \tag{2.9}$$

$$\boldsymbol{\omega} = \omega_x\mathbf{i} + \omega_y\mathbf{j} + \omega_z\mathbf{k} \tag{2.10}$$

$$\mathbf{H} = H_x\mathbf{i} + H_y\mathbf{j} + H_z\mathbf{k} \tag{2.11}$$

$$\boldsymbol{\tau} = L\mathbf{i} + M\mathbf{j} + N\mathbf{k}. \tag{2.12}$$

On substituting these into (2.7) we obtain

$$\mathbf{H} = \mathsf{J}\boldsymbol{\omega}, \tag{2.13}$$

where J is a constant, symmetric matrix called *inertia tensor*, given by:

$$\mathsf{J} \doteq \begin{pmatrix} \int (y^2 + z^2)\mathrm{d}m & -\int xy\mathrm{d}m & -\int xz\mathrm{d}m \\ -\int xy\mathrm{d}m & \int (x^2 + z^2)\mathrm{d}m & -\int yz\mathrm{d}m \\ -\int xz\mathrm{d}m & -\int yz\mathrm{d}m & \int (x^2 + y^2)\mathrm{d}m \end{pmatrix}. \tag{2.14}$$

In terms of its components, J is written as follows:

$$\mathsf{J} \doteq \begin{pmatrix} J_{xx} & J_{xy} & J_{xz} \\ J_{xy} & J_{yy} & J_{yz} \\ J_{xz} & J_{yz} & J_{zz} \end{pmatrix}. \tag{2.15}$$

The components of the inertia tensor are divided into the *moments of inertia*, J_{xx}, J_{yy}, J_{zz}, and the *products of inertia*, J_{xy}, J_{yz}, J_{xz}. As the inertia tensor accounts for the mass distribution of the body, it is clear from (2.13) that the way mass is distributed in a vehicle is crucial to rotational flight dynamics.

The final step in our derivation of rotational kinetics equations is to express the inertial time derivative of (2.13) relative to the rotating body-fixed frame as follows:

$$\boldsymbol{\tau} = \mathsf{J}\dot{\boldsymbol{\omega}} + \boldsymbol{\omega} \times (\mathsf{J}\boldsymbol{\omega}), \tag{2.16}$$

where, as previously, the overdot represents the partial time derivative taken with reference to the body-fixed frame,

$$\dot{\boldsymbol{\omega}} \doteq \begin{Bmatrix} \dfrac{\mathrm{d}\omega_x}{\mathrm{d}t} \\ \dfrac{\mathrm{d}\omega_y}{\mathrm{d}t} \\ \dfrac{\mathrm{d}\omega_z}{\mathrm{d}t} \end{Bmatrix} = \begin{Bmatrix} \dot{\omega}_x \\ \dot{\omega}_y \\ \dot{\omega}_z \end{Bmatrix}. \tag{2.17}$$

By replacing the vector product in (2.16) by a matrix product, we have

$$\boldsymbol{\tau} = \mathsf{J}\dot{\boldsymbol{\omega}} + \mathsf{S}(\boldsymbol{\omega})\mathsf{J}\boldsymbol{\omega}, \tag{2.18}$$

where

$$\mathsf{S}(\boldsymbol{\omega}) = \begin{pmatrix} 0 & -\omega_z & \omega_y \\ \omega_z & 0 & -\omega_x \\ -\omega_y & \omega_x & 0 \end{pmatrix} \tag{2.19}$$

is a *skew-symmetric* matrix. Equation (2.18) represents three scalar, coupled, nonlinear, ordinary differential equations, and are called *Euler's equations* of rotational kinetics, whose solution gives the angular velocity, $\boldsymbol{\omega}$, at a given time.

2.3 Attitude Kinematics

In many cases, the rotation of a flight vehicle is important in itself for various reasons (aerodynamics, pointing of weapons, payload, or antennas, etc.), and governs the intantaneous *attitude* (orientation) of the vehicle. The vehicle's attitude is given by the orientation of the body-fixed frame (*oxyz*) relative to a reference frame (*oXYZ*). The time dependence of a frame's orientation relative to another frame is termed *rotational kinematics*, and can be described using the coordinate transformation between the two frames.

Let us represent the axes *ox, oy, oz* of the rotating frame, (*oxyz*), by the unit vectors $\mathbf{i}, \mathbf{j}, \mathbf{k}$, respectively. The orientation of (*oxyz*) relative to the reference frame (*oXYZ*) – whose axes *oX, oY, oZ* are represented by the unit triad $\mathbf{I}, \mathbf{J}, \mathbf{K}$ – is given by the following coordinate transformation:

$$\begin{Bmatrix} \mathbf{i} \\ \mathbf{j} \\ \mathbf{k} \end{Bmatrix} = \mathsf{C} \begin{Bmatrix} \mathbf{I} \\ \mathbf{J} \\ \mathbf{K} \end{Bmatrix}, \tag{2.20}$$

where C is called the *rotation matrix*. A rotation matrix is *orthogonal*, i.e., it satisfies $\mathsf{C}^{\mathrm{T}}\mathsf{C} = \mathsf{C}\mathsf{C}^{\mathrm{T}} = \mathsf{I}$. Furthermore, the determinant of a rotation matrix is unity. Associated with the rotation matrix is the concept of *Euler axis* and the *principal angle*. *Euler's theorem* states that the relative orientation of any pair of coordinate frames is uniquely determined by a rotation by angle, Φ, called the principal angle about a fixed axis through the common origin of the two frames, called Euler axis and denoted by the unit vector $\mathbf{e}$. As Euler axis is invariant under coordinate frame rotation, it can be shown that $\mathbf{e}$ is the eigenvector of C corresponding to a unity eigenvalue, and hence satisfies $\mathsf{C}\mathbf{e} = \mathbf{e}$. Similarly, it can be also shown that the principal angle satisfies the equation $\cos\Phi = \frac{1}{2}(trace\mathsf{C} - 1)$.

The rotational kinematics equation can be derived by differentiating with time both the sides of (2.20), thereby producing

$$\begin{Bmatrix} \boldsymbol{\omega} \times \mathbf{i} \\ \boldsymbol{\omega} \times \mathbf{j} \\ \boldsymbol{\omega} \times \mathbf{k} \end{Bmatrix} = \frac{\mathrm{d}\mathsf{C}}{\mathrm{d}t} \begin{Bmatrix} \mathbf{I} \\ \mathbf{J} \\ \mathbf{K} \end{Bmatrix}, \tag{2.21}$$

or, using the matrix product of (2.18), we have

$$-\mathsf{S}(\boldsymbol{\omega}) \begin{Bmatrix} \mathbf{i} \\ \mathbf{j} \\ \mathbf{k} \end{Bmatrix} = \frac{\mathrm{d}\mathsf{C}}{\mathrm{d}t}\mathsf{C}^{\mathrm{T}} \begin{Bmatrix} \mathbf{i} \\ \mathbf{j} \\ \mathbf{k} \end{Bmatrix}, \tag{2.22}$$

from which (along with the orthogonality of C) it follows that

$$\frac{\mathrm{d}\mathsf{C}}{\mathrm{d}t} = -\mathsf{S}(\boldsymbol{\omega})\mathsf{C}(t). \tag{2.23}$$

Equation (2.23) is the governing equation of attitude kinematics. Because the rotation matrix corresponding to a particular attitude can be represented by several alternative kinematic parameters (such as *Euler angles* and *quaternion* to be considered later), the attitude kinematics equation can be expressed in terms of various parameters. It is interesting to note the following definition of the angular velocity of a frame in terms of Euler axis and incremental principal angle, $\Delta\Phi$

$$\boldsymbol{\omega}(t) \doteq \lim_{\Delta t \to 0} \frac{\Delta\Phi\mathbf{e}}{\Delta t}. \tag{2.24}$$

As noted earlier, one can employ various alternative descriptions of the rotation matrix, called attitude representations. We will consider next the attitude representations commonly used in flight control applications – namely, Euler angles and quaternion. Each attitude representation has its advantages and disadvantages, and is suited to a particular flight situation. For example, Euler angles are best suited to small rotations of flight vehicles about their equilibrium orientation, while quaternion can handle large, multiaxis rotations that are often encountered in extreme flight maneuvers.

2.3.1 Euler Angles

Euler angles are based on the fact that a general orientation of a coordinate frame can be obtained by using successive rotations about the axes of the frame. Rotation of a frame about one of its axes is called an *elementary rotation*. The largest number of such rotations needed to uniquely specify a given orientation, called rotational *degrees of freedom*, is three. Hence, we can employ three angles, each about a particular coordinate axis, to describe a given orientation. Such a representation of the attitude by three elementary rotations is called an Euler angle representation, and the concerned angles are known as Euler angles.

An *anticlockwise* rotation is considered positive by the right-hand rule. A positive elementary rotation of the frame $(oXYZ)$ about oX by angle Φ is given by the rotation matrix

$$\mathsf{C}_1 \doteq \begin{pmatrix} 1 & 0 & 0 \\ 0 & \cos\Phi & \sin\Phi \\ 0 & -\sin\Phi & \cos\Phi \end{pmatrix}, \tag{2.25}$$

whereas, the rotation matrix for a positive rotation about oY by the same angle is

$$\mathsf{C}_2 \doteq \begin{pmatrix} \cos\Phi & 0 & -\sin\Phi \\ 0 & 1 & 0 \\ \sin\Phi & 0 & \cos\Phi \end{pmatrix}. \tag{2.26}$$

Similarly, a positive rotation about oZ by Φ is given by:

$$\mathsf{C}_3 \doteq \begin{pmatrix} \cos\Phi & \sin\Phi & 0 \\ -\sin\Phi & \cos\Phi & 0 \\ 0 & 0 & 1 \end{pmatrix}. \tag{2.27}$$

One can easily verify the orthogonality of the rotation matrix for each of the elementary rotations.

The sequence of elementary rotations is of utmost importance in the Euler angle representation. We can specify the Euler angles and the axes of elementary rotations using notation such as $(\Psi)_3, (\Theta)_2, (\sigma)_1$ shown in the right diagram of Fig. 2.2. This particular representation consists of a rotation of $(\mathbf{I}, \mathbf{J}, \mathbf{K})$ by angle Ψ about $\mathbf{K}$, resulting in the intermediate orientation, $(\mathbf{I}', \mathbf{J}', \mathbf{K})$, followed by a rotation by angle Θ about $\mathbf{J}'$, thereby producing $(\mathbf{I}'', \mathbf{J}', \mathbf{K}'')$. Finally, a rotation by angle σ about $\mathbf{I}''$, yields the desired attitude, $(\mathbf{i}, \mathbf{j}, \mathbf{k})$. The $(\Psi)_3, (\Theta)_2, (\sigma)_1$ representation is commonly used for describing an aircraft's attitude relative to a local horizontal frame using the Euler angles, yaw (Ψ), pitch (Θ), and roll (σ). An alternative Euler representation employed in spacecraft orientation is the Euler sequence $(\Psi)_3, (\Theta)_1, (\sigma)_3$, shown on the left side of Fig. 2.2. It is clear from Fig. 2.2 that the Euler representations are not unique (i.e., different Euler angle sequences can be employed to represent the same attitude).

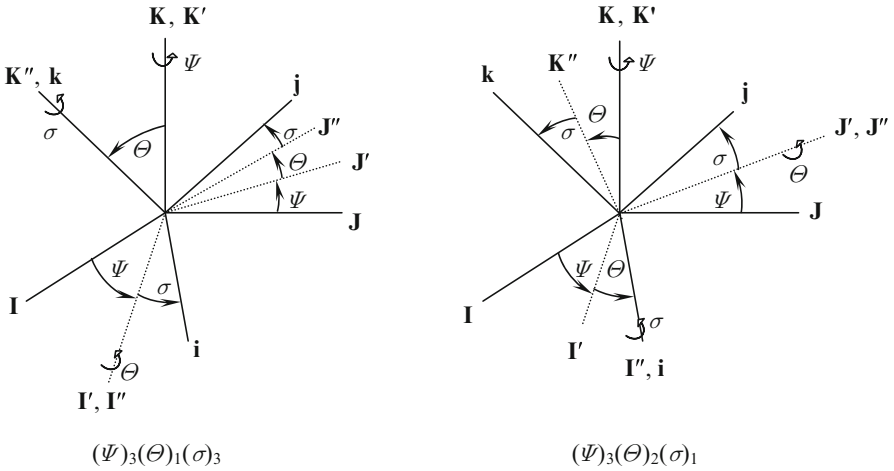

Fig. 2.2 The Euler angle representations, $(\Psi)_3, (\Theta)_1, (\sigma)_3$ and $(\Psi)_3, (\Theta)_2, (\sigma)_1$

The rotation matrix relating the final orientation of *(oxyz)* to *(oXYZ)* for the Euler angle representation $(\Psi)_3, (\Theta)_1, (\sigma)_3$ is given by:

$$\begin{aligned} \mathsf{C} &= \mathsf{C}_3(\sigma)\mathsf{C}_1(\Theta)\mathsf{C}_3(\Psi) \\ &= \begin{pmatrix} (\cos\Psi\cos\sigma - \sin\Psi\sin\sigma\cos\Theta) & (\sin\Psi\cos\sigma + \cos\Psi\sin\sigma\cos\Theta) & \sin\sigma\sin\Theta \\ -(\cos\Psi\sin\sigma + \sin\Psi\cos\sigma\cos\Theta) & (-\sin\Psi\sin\sigma + \cos\Psi\cos\sigma\cos\Theta) & \cos\sigma\sin\Theta \\ \sin\Psi\sin\Theta & -\cos\Psi\sin\Theta & \cos\Theta \end{pmatrix} \end{aligned} \tag{2.28}$$

Similarly, the rotation matrix for the orientation $(\Psi)_3, (\Theta)_2, (\sigma)_1$ is the following:

$$\begin{aligned} \mathsf{C} &= \mathsf{C}_1(\sigma)\mathsf{C}_2(\Theta)\mathsf{C}_3(\Psi) \\ &= \begin{pmatrix} \cos\Theta\cos\Psi & \cos\Theta\sin\Psi & -\sin\Theta \\ (\sin\sigma\sin\Theta\cos\Psi - \cos\sigma\sin\Psi) & (\sin\sigma\sin\Theta\sin\Psi + \cos\sigma\cos\Psi) & \sin\sigma\cos\Theta \\ (\cos\sigma\sin\Theta\cos\Psi + \sin\sigma\sin\Psi) & (\cos\sigma\sin\Theta\sin\Psi - \sin\sigma\cos\Psi) & \cos\sigma\cos\Theta \end{pmatrix} \end{aligned} \tag{2.29}$$

Note that the rotation matrix given by (2.28) becomes the following when $\sin\Theta = 0$:

$$\mathsf{C} = \begin{pmatrix} \cos(\sigma \pm \Psi) & \sin(\sigma \pm \Psi) & 0 \\ \mp\sin(\sigma \pm \Psi) & \pm\cos(\sigma \pm \Psi) & 0 \\ 0 & 0 & \pm 1 \end{pmatrix}, \tag{2.30}$$

which shows that the angles σ and Ψ cannot be resolved from the rotation matrix, but only their sum (or difference) can be determined. Such special orientations for which Euler angles become ambiguous are called *singularities*. Thus, the representation $(\Psi)_3, (\Theta)_1, (\sigma)_3$ has singularities at $\Theta = n\pi,\ (n = 0, 1, 2, 3, \ldots)$, and the representation is thus limited to rotations of $0 \leq \Theta < \pi$ that generally apply to spacecraft attitudes. Similarly, it can be shown that the Euler angle representation $(\Psi)_3, (\Theta)_2, (\sigma)_1$ has singularities at $\Theta = n\frac{\pi}{2}$, $(n = 0, 1, 3, \ldots)$, which limits the utility of the representation to rotations involving $\pi/2 \leq \Theta < \pi/2$. From the singularities and the resulting domain of applicability of a particular Euler angle representation one can derive its application. In any case, Euler angles cannot be used for rotations of principal angle greater than 180°. For attitudes that do not lead to singularities in an Euler angle representation, the three angles can be unambiguously determined from the rotation matrix.

The differential equations governing attitude kinematics can be easily derived for Euler angles by employing the appropriate rotation matrix and expressing the angular velocity in terms of the angular rates. For example, using the $(\Psi)_3, (\Theta)_1, (\sigma)_3$ representation we can write the angular velocity, $\boldsymbol{\omega}(t)$, as follows:

$$\boldsymbol{\omega}(t) = \dot{\sigma}\mathbf{k} + \dot{\Theta}\mathbf{I}' + \dot{\Psi}\mathbf{K}, \tag{2.31}$$

which, considering the elementary rotations involved in (2.28), becomes

$$\boldsymbol{\omega}(t) = \begin{Bmatrix} \omega_x \\ \omega_y \\ \omega_z \end{Bmatrix} = \begin{Bmatrix} \dot{\Psi}\sin\sigma\sin\Theta + \dot{\Theta}\cos\sigma \\ \dot{\Psi}\cos\sigma\sin\Theta - \dot{\Theta}\sin\sigma \\ \dot{\Psi}\cos\Theta + \dot{\sigma} \end{Bmatrix}, \tag{2.32}$$

or,

$$\begin{Bmatrix} \dot{\Psi} \\ \dot{\Theta} \\ \dot{\sigma} \end{Bmatrix} = \frac{1}{\sin\Theta} \begin{pmatrix} \sin\sigma & \cos\sigma & 0 \\ \cos\sigma\sin\Theta & -\sin\sigma\sin\Theta & 0 \\ -\sin\sigma\cos\Theta & -\cos\sigma\cos\Theta & \sin\Theta \end{pmatrix} \begin{Bmatrix} \omega_x \\ \omega_y \\ \omega_z \end{Bmatrix}. \tag{2.33}$$

Equation (2.33) is the required set of kinematical equations, and clearly indicates the singularities of the particular representation for $\sin\Theta = 0$.

2.3.2 *Quaternion*

Any attitude representation based upon only three kinematic parameters (such as Euler angles) is bound to be singular. For a universal application, we desire a nonsingular representation. It can be easily shown that the four parameter system of Euler axis, $\mathbf{e}$, and principal angle, Φ, is one such nonsingular attitude representation. Another four parameter, nonsingular attitude representation that is closely related to Euler axis/principal angle combination is the *quaternion* representation. The attitude

quaternion is a special set composed of four mutually dependent scalar parameters, q_1, q_2, q_3, q_4, such that the first three form a vector, called the *vector part*,

$$\mathbf{q} \doteq \begin{Bmatrix} q_1 \\ q_2 \\ q_3 \end{Bmatrix}, \tag{2.34}$$

and the fourth, q_4, represents the *scalar part*. The quaternion for attitude representation can be derived from the Euler axis, $\mathbf{e}$, and principal rotation angle, Φ, as follows:

$$\begin{aligned} q_i &\doteq e_i \sin\frac{\Phi}{2} \quad (i = 1, 2, 3) \\ q_4 &\doteq \cos\frac{\Phi}{2}. \end{aligned} \tag{2.35}$$

It is clear from (2.35) that q_1, q_2, q_3, q_4, must satisfy the constraint equation,

$$q_1^2 + q_2^2 + q_3^2 + q_4^2 = 1. \tag{2.36}$$

This constraint implies that the quaternion yields only three independent, scalar parameters, as in the principal angle/Euler axis, or the Euler angle representations. As the four elements of the quaternion satisfy the constraint equation, (2.36), it can be said that attitude orientations vary along the surface of a *four-dimensional* unit sphere without any singularity. The chief advantage of the quaternion over the principal angle/Euler axis combination (also a nonsingular representation) lies in that the former does not require computationally intensive trigonometric function evaluations when derived from the rotation matrix.

The rotation matrix, C, can be written in terms of the quaternion as follows:

$$\mathsf{C} = (q_4^2 - \mathbf{q}^{\mathrm{T}}\mathbf{q})\mathsf{I} + 2\mathbf{q}\mathbf{q}^{\mathrm{T}} - 2q_4\mathsf{S}(\mathbf{q}), \tag{2.37}$$

where $\mathsf{S}(\mathbf{q})$ is the following skew-symmetric matrix function formed out of the elements of vector $\mathbf{q}$:

$$\mathsf{S}(\mathbf{q}) = \begin{pmatrix} 0 & -q_3 & q_2 \\ q_3 & 0 & -q_1 \\ -q_2 & q_1 & 0 \end{pmatrix}. \tag{2.38}$$

We can write (2.37) in terms of the individual quaternion elements as follows:

$$\mathsf{C} = \begin{pmatrix} q_1^2 - q_2^2 - q_3^2 + q_4^2 & 2(q_1q_2 + q_3q_4) & 2(q_1q_3 - q_2q_4) \\ 2(q_1q_2 - q_3q_4) & -q_1^2 + q_2^2 - q_3^2 + q_4^2 & 2(q_2q_3 + q_1q_4) \\ 2(q_1q_3 + q_2q_4) & 2(q_2q_3 - q_1q_4) & -q_1^2 - q_2^2 + q_3^2 + q_4^2 \end{pmatrix}, \tag{2.39}$$

which yields the following expressions for calculating the quaternion elements from the elements of the rotation matrix, c_{ij}:

$$\begin{aligned} q_1 &= \frac{c_{23} - c_{32}}{4q_4} \\ q_2 &= \frac{c_{31} - c_{13}}{4q_4} \\ q_3 &= \frac{c_{12} - c_{21}}{4q_4}, \end{aligned} \tag{2.40}$$

where

$$q_4 = \pm\frac{1}{2}\sqrt{1 + c_{11} + c_{22} + c_{33}} = \pm\frac{1}{2}\sqrt{1 + trace\mathsf{C}}. \tag{2.41}$$

Equation (2.41) implies that the quaternion representation is nonunique (eventhough C is free from such an ambiguity). The sign ambiguity in determining the quaternion can be physically understood by the fact that a rotation by angle Φ about an axis $\mathbf{e}$ is the same as a rotation by $-\Phi$ about $-\mathbf{e}$. As there is no loss of generality in always taking a particular sign in (2.41), doing so removes the ambiguity in the quaternion representation. Of course, the derivation given earlier is valid only if $q_4 \neq 0$. If q_4 is close to zero, one can employ an alternative derivation, such as the following:

$$\begin{aligned} q_2 &= \frac{c_{12} + c_{21}}{4q_1} \\ q_3 &= \frac{c_{31} + c_{13}}{4q_1} \\ q_4 &= \frac{c_{23} - c_{32}}{4q_1}, \end{aligned} \tag{2.42}$$

where

$$q_1 = \pm\frac{1}{2}\sqrt{1 + c_{11} - c_{22} - c_{33}}. \tag{2.43}$$

Other alternative derivations of the quaternion from the rotation matrix involve a similar division by either q_2 or q_3.

The most useful feature of the quaternion representation for a frame's attitude is the rather simple *composition rule* by which successive rotations can be combined, given by:

$$\mathsf{C}(\mathbf{q}'', q_4'') = \mathsf{C}(\mathbf{q}', q_4')\mathsf{C}(\mathbf{q}, q_4), \tag{2.44}$$

or,

$$\begin{Bmatrix} q_1'' \\ q_2'' \\ q_3'' \\ q_4'' \end{Bmatrix} = \begin{pmatrix} q_4' & q_3' & -q_2' & q_1' \\ -q_3' & q_4' & q_1' & q_2' \\ q_2' & -q_1' & q_4' & q_3' \\ -q_1' & -q_2' & -q_3' & q_4' \end{pmatrix} \begin{Bmatrix} q_1 \\ q_2 \\ q_3 \\ q_4 \end{Bmatrix}. \tag{2.45}$$

The composition rule of (2.45) is the defining property of the quaternion. In fact, any four parameter set obeying (2.45) is termed the quaternion, of which the attitude quaternion of (2.35) is a special subset.

By substituting (2.35) for an infinitesimal rotation into (2.24), the attitude kinematics equation (2.23) can be expressed in terms of the quaternion as follows:

$$\frac{\mathrm{d}\{\mathbf{q}, q_4\}^{\mathrm{T}}}{\mathrm{d}t} = \frac{1}{2}\Omega\{\mathbf{q}(t), q_4(t)\}^{\mathrm{T}}, \tag{2.46}$$

where

$$\Omega = \begin{pmatrix} 0 & \omega_z & -\omega_y & \omega_x \\ -\omega_z & 0 & \omega_x & \omega_y \\ \omega_y & -\omega_x & 0 & \omega_z \\ -\omega_x & -\omega_y & -\omega_z & 0 \end{pmatrix}. \tag{2.47}$$

The linear, algebraic form of the attitude kinematics equation, (2.47), is an obvious advantage of the quaternion representation over the nonlinear, transcendental kinematics equation (such as (2.33)) of an Euler angle representation.

The main disadvantage of the quaternion attitude representation is its redundancy, which causes an attitude to be represented by more than one quaternion and sometimes leads to practical problems when employed in a flight control system. In order to remove redundancy, the quaternion is often replaced by a closely related, three parameter set such as either the *Rodrigues* or the *modified Rodrigues* parameters. However, being three parameter representations like the Euler angles, such minimal representations suffer from inherent singularities, and thus can be applied in a limited range of principal angles.

2.4 Flight Dynamics

As noted earlier, flight dynamics consists of translation of the center of mass (2.2) and rotation of the vehicle about the center of mass (2.8). Therefore, flight dynamics can be separated into translational flight dynamics and rotational dynamics (also called *attitude dynamics*). Generally, translational flight dynamics deals with the motion of the center of mass in a reference frame at the center of a celestial body (e.g., Earth, Sun, Moon, other planets), and attitude dynamics refers to the rotation of a body-fixed frame about the center of mass of the vehicle. The attitude (or orientation) of the body-fixed frame is generally measured relative to a third coordinate frame.

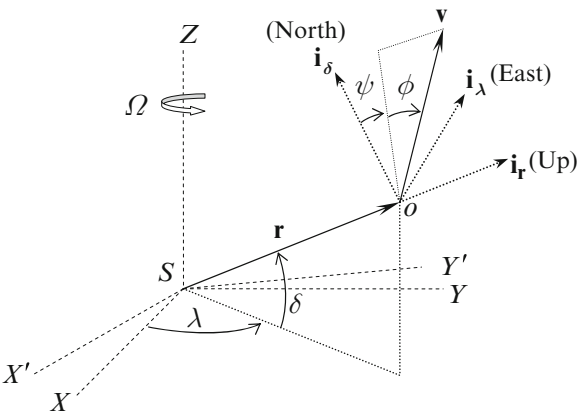

Fig. 2.3 Planet-fixed frame and the inertial reference frame

2.4.1 Translational Kinematics in Planet-Fixed Frame

For the purpose of long-range guidance and navigation, the equations of translational kinematics are resolved in a reference frame fixed to the planet, with origin at planetary center.

Consider a reference frame $(SXYZ)$ rigidly fixed to the center of a planet and rotating with it (Fig. 2.3), with the axes given by the unit vectors $\mathbf{I}, \mathbf{J}, \mathbf{K}$, respectively. The angular velocity of $(SXYZ)$ relative to a stationary frame, $(SX'Y'Z)$, at the center of the planet is given by $\boldsymbol{\Omega} = \Omega\mathbf{K}$. The instantaneous position, $\mathbf{r}(t)$, of the flight vehicle's center of mass, o, is resolved in $(SXYZ)$ using the spherical coordinates $(r(t), \lambda(t), \delta(t))$ denoting the radius, longitude, and latitude, respectively. The velocity vector is represented by another set of spherical coordinates, $(v(t), \phi(t), \psi(t))$, resolved in a moving frame called *local horizon frame* with axes $\mathbf{i}_\mathbf{r}, \mathbf{i}_\lambda, \mathbf{i}_\delta$ representing the local directions, vertical (*Up*), *East*, and *North*, respectively, as shown in Fig. 2.4. Here, $\phi(t)$ is the *flight path angle*, and $\psi(t)$ is the *heading angle* (or *velocity azimuth*). The *relative velocity*, $\mathbf{v}(t)$, is expressed as follows:

$$\mathbf{v} = v\left(\sin\phi\mathbf{i}_\mathbf{r} + \cos\phi\sin\psi\mathbf{i}_\lambda + \cos\phi\cos\psi\mathbf{i}_\delta\right), \tag{2.48}$$

and the coordinate transformation between the planet-fixed and the local horizon frames is given by Euler angle sequence $(\lambda)_3, (-\delta)_2$ as follows:

$$\begin{Bmatrix} \mathbf{i}_\mathbf{r} \\ \mathbf{i}_\lambda \\ \mathbf{i}_\delta \end{Bmatrix} = \mathsf{C}_{\mathsf{LH}} \begin{Bmatrix} \mathbf{I} \\ \mathbf{J} \\ \mathbf{K} \end{Bmatrix}, \tag{2.49}$$

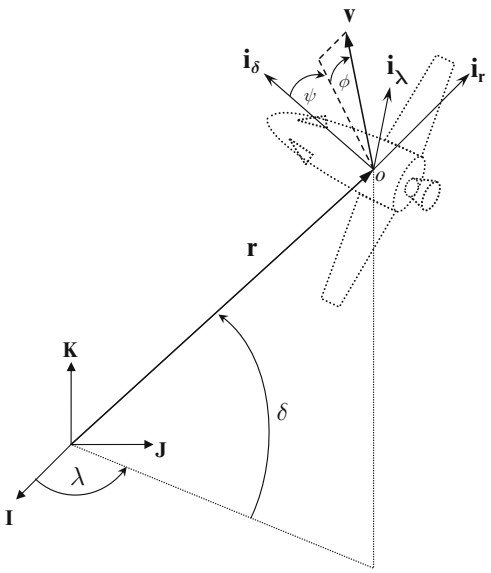

Fig. 2.4 The planet-fixed frame, $(\mathbf{I}, \mathbf{J}, \mathbf{K})$, and the local horizon frame, $(\mathbf{i}_\mathbf{r}, \mathbf{i}_{\boldsymbol{\lambda}}, \mathbf{i}_{\boldsymbol{\delta}})$

where

$$\mathsf{C}_{\mathsf{LH}} = \mathsf{C}_2(-\delta)\mathsf{C}_3(\lambda) = \begin{pmatrix} \cos\delta\cos\lambda & \cos\delta\sin\lambda & \sin\delta \\ -\sin\lambda & \cos\lambda & 0 \\ -\sin\delta\cos\lambda & -\sin\delta\sin\lambda & \cos\delta \end{pmatrix}. \tag{2.50}$$

With planetary angular velocity, $\boldsymbol{\Omega} = \Omega\mathbf{K}$, and the angular velocity of the local horizon frame relative to the planet-fixed frame given by:

$$\boldsymbol{\Omega}_{LH} = \dot{\lambda}\mathbf{K} - \dot{\delta}\mathbf{i}_{\boldsymbol{\lambda}} = \dot{\lambda}\sin\delta\mathbf{i}_\mathbf{r} - \dot{\delta}\mathbf{i}_{\boldsymbol{\lambda}} + \dot{\lambda}\cos\delta\mathbf{i}_{\boldsymbol{\delta}}, \tag{2.51}$$

we can express the relative and inertial velocities, $\mathbf{v}(t), \mathbf{v}_\mathbf{I}(t)$, respectively, as follows:

$$\mathbf{v} = \dot{h}\mathbf{i}_\mathbf{r} + (R_0 + h)(\dot{\lambda}\cos\delta\mathbf{i}_{\boldsymbol{\lambda}} + \dot{\delta}\mathbf{i}_{\boldsymbol{\delta}}), \tag{2.52}$$

$$\mathbf{v}_\mathbf{I} = \mathbf{v} + \Omega(R_0 + h)\cos\delta\mathbf{i}_{\boldsymbol{\lambda}}. \tag{2.53}$$

Here, $r(t) = R_0 + h(t)$ is the radial coordinate of the center of mass, with R_0 being the (constant) radius of the spherical planet and $h(t)$, the instantaneous altitude.

Comparing (2.52) with (2.48) we have the following translational kinematics equations:

$$\dot{h} = v\sin\phi, \tag{2.54}$$

$$\dot{\delta} = \frac{v \cos\phi \cos\psi}{R_0 + h}, \tag{2.55}$$

$$\dot{\lambda} = \frac{v \cos\phi \sin\psi}{(R_0 + h)\cos\delta}. \tag{2.56}$$

2.4.2 Attitude Flight Dynamics

The flight vehicle is often considered to be a collection of rigid bodies rotating with respect to one another. The outer frame of the vehicle thus contains a number of rotors spinning with respect to the vehicle about various axes. Using the body-fixed frame with origin at vehicle's center of mass, $(\mathbf{i}, \mathbf{j}, \mathbf{k})$, we can resolve the net angular momentum of the vehicle as follows:

$$\mathbf{H} = \mathsf{J}\boldsymbol{\omega} + \mathbf{H_R} = \begin{pmatrix} J_{xx} & J_{xy} & J_{xz} \\ & J_{yy} & J_{yz} \\ Symm. & & J_{zz} \end{pmatrix} \begin{Bmatrix} P \\ Q \\ R \end{Bmatrix} + \begin{Bmatrix} H_{Rx} \\ H_{Ry} \\ H_{Rz} \end{Bmatrix}, \tag{2.57}$$

where $\mathbf{H_R} = H_{Rx}\mathbf{i} + H_{Ry}\mathbf{j} + H_{Rz}\mathbf{k}$ is the net (constant) angular momentum of all rotors relative to the vehicle frame. Writing the external torque vector in the body-fixed frame as:

$$\boldsymbol{\tau} = L\mathbf{i} + M\mathbf{j} + N\mathbf{k}, \tag{2.58}$$

and substituting (2.57) and (2.58) into (2.16), we have the following rotational kinetics equation:

$$\begin{Bmatrix} L \\ M \\ N \end{Bmatrix} = \mathsf{J} \begin{Bmatrix} \dot{P} \\ \dot{Q} \\ \dot{R} \end{Bmatrix} + \begin{Bmatrix} P \\ Q \\ R \end{Bmatrix} \times \left(\mathsf{J} \begin{Bmatrix} P \\ Q \\ R \end{Bmatrix} + \begin{Bmatrix} H_{Rx} \\ H_{Ry} \\ H_{Rz} \end{Bmatrix} \right). \tag{2.59}$$

Typically, the rotor angular momentum is negligible for aircraft and rockets, but can be significant for a spacecraft. Note that rotational kinetic equations have constant (equilibrium) solutions for the body rates P, Q, R when the external torque vanishes, $\mathbf{H_R}$ is constant, and any two body rates are zeros. Such equilibrium solutions are commonly employed in the design of flight control systems. Other equilibrium solutions are torque-free rotation of axisymmetric vehicles about their axis of symmetry, which form the basis of spin stabilization of rockets and spacecraft. For example, axisymmetric rockets can roll at a constant rate, P^{e}, but with zero pitch and yaw rates. On the other hand, airplanes and asymmetric satellites in horizontal flight can have a constant pitch rate, Q^{e}, but zero roll and yaw rates.

The rotational kinematics equation can be derived from (2.23) with the help of a suitable attitude representation, as discussed earlier. Usually, rotational stability

analysis requires a small angular displacement from a nominal attitude. In such a case, the attitude perturbation is represented by $(\Psi)_3, (\Theta)_2, (\sigma)_1$ Euler sequence (Fig. 2.2), where the angles Ψ, Θ, σ are small. When the small attitude perturbation is measured with reference to an axis normal to the nominal attitude, the $(\Psi)_3, (\Theta)_1, (\sigma)_3$ representation (Fig. 2.2) is used. In both cases, linearized models of attitude kinematics are possible. However, for an arbitrarily large perturbation, a nonsingular representation (such as quaternion) is necessary, resulting in an essentially nonlinear model.

2.5 Flight Dynamics System

We can now collect the equations of motion of a generic, rigid flight vehicle in a reference frame rotating with a constant angular velocity, $\mathbf{\Omega}$, in terms of position, $\mathbf{r}(t)$, and velocity, $\mathbf{v}(t)$, of the center of mass, o, as well as angular velocity, $\boldsymbol{\omega}(t)$, and rotation matrix defining angular orientation, $\mathsf{C}(t)$. The external force and moment vectors are expressed in terms of the contributing effects of control $(\mathbf{F_C}(t),\ \mathbf{M_C}(t))$, environment $(\mathbf{F_E}(t),\ \boldsymbol{\tau}_\mathbf{E}(t))$, and disturbance $(\mathbf{F_D}(t),\ \boldsymbol{\tau}_\mathbf{D}(t))$ as follows:

$$\mathbf{v} = \frac{\mathrm{d}\mathbf{r}}{\mathrm{d}t} = \dot{\mathbf{r}}_\mathbf{o} + \mathbf{\Omega} \times \mathbf{r}. \tag{2.60}$$

$$\mathbf{F_C} + \mathbf{F_D} + \mathbf{F_E} = m\frac{\mathrm{d}\mathbf{v}}{\mathrm{d}t} = m\left(\dot{\mathbf{v}}_\mathbf{o} + \mathbf{\Omega} \times \mathbf{v}\right). \tag{2.61}$$

$$\boldsymbol{\tau}_\mathbf{C} + \boldsymbol{\tau}_\mathbf{E} + \boldsymbol{\tau}_\mathbf{D} = \mathsf{J}\dot{\boldsymbol{\omega}} + \mathsf{S}(\boldsymbol{\omega})\mathsf{J}\boldsymbol{\omega}. \tag{2.62}$$

$$\frac{\mathrm{d}\mathsf{C}}{\mathrm{d}t} = -\mathsf{S}(\boldsymbol{\omega})\mathsf{C}(t). \tag{2.63}$$

Here, overdot represents time derivative. The mass, m, and the inertia tensor, J, of the vehicle could be changing with time due to propellant consumption, and the respective thrust and torque terms due to varying mass and mass distribution are assumed to be included in the environmental effects on the left-hand side of (2.61) and (2.62). Although the general attitude kinematics equation, (2.63), has been expressed in terms of the rotation matrix, it is more convenient in practice to use a generic parameter vector, $\boldsymbol{\xi}(t)$, that could be a set of Euler angles, quaternion, or any other attitude kinematical representation. Assuming that the environmental, control, and distrubance inputs are known, the equations of motion, (2.60)–(2.63), can be completely described by the variables of motion, $\mathbf{r},\ \mathbf{v},\ \boldsymbol{\omega},\ \boldsymbol{\xi}$. Thus, we can represent the state of the flight dynamic system by the state vector, $\boldsymbol{\zeta}(t)$, given by:

$$\boldsymbol{\zeta}(t) = \begin{Bmatrix} \mathbf{r}(t) \\ \mathbf{v}(t) \\ \boldsymbol{\omega}(t) \\ \boldsymbol{\xi}(t) \end{Bmatrix}. \tag{2.64}$$

The state vector is not unique, but depends upon the choice of frames of reference in the equations of motion. Any vector can be resolved in a variety of coordinate frames, resulting in different scalar differential equations of motion for the same flight vehicle.

The environmental inputs arise because of sustained flight in a given environment (either atmosphere or space). The environmental effects are described by additional equations – called environmental equations – involving functions of the state vector, $\boldsymbol{\zeta}(t)$, and time, written in a vector form as follows:

$$\begin{Bmatrix} \mathbf{F_E}(t) \\ \boldsymbol{\tau}_\mathbf{E}(t) \end{Bmatrix} = \mathbf{f_e}(\boldsymbol{\zeta}(t), t), \tag{2.65}$$

where $\mathbf{f_e}(.)$ is the environmental vector functional. In atmospheric flight, the environmental force, $\mathbf{F_E}$, is a sum of gravity, $\mathbf{F_g}$, thrust, $\mathbf{F_t}$, and aerodynamic force, $\mathbf{F_a}$, while the aerodynamic moment $\boldsymbol{\tau}_\mathbf{a}$ is the only environmental torque. In space flight, the typical environmental effects are gravity, solar-radiation pressure (force and torque, $\mathbf{F_s}$, $\boldsymbol{\tau}_\mathbf{s}$), third-body and nonspherical gravity force, $\mathbf{F_{\delta g}}$, gravity-gradient torque, $\boldsymbol{\tau}_\mathbf{g}$, and aerodynamic force and moment in rarefied flow ($\mathbf{F_a}$, $\boldsymbol{\tau}_\mathbf{a}$).

Often, it is not feasible to model all environmental effects as deterministic processes. Examples include random atmospheric gusts and sloshing of propellants. In such cases, some environmental effects are treated as disturbance forces and moments ($\mathbf{F_D}$, $\boldsymbol{\tau}_\mathbf{D}$), and are generally treated as stochastic (statistical) processes. The disturbance inputs include errors (or uncertainty) in modeling the flight dynamic system due to idealizing assumptions (such as rigid body approximation). Therefore, all disturbances in the flight dynamics model are clubbed into the *process noise* vector, $\boldsymbol{\nu}(t)$, that is modeled as a stochastic input:

$$\boldsymbol{\nu}(t) \doteq \begin{Bmatrix} \mathbf{F_D}(t) \\ \boldsymbol{\tau}_\mathbf{D}(t) \end{Bmatrix}. \tag{2.66}$$

Finally, control inputs are required either to maintain a nominal trajectory in presence of disturbances or to achieve a change of state in a given time. The control input vector,

$$\mathbf{u}(t) \doteq \begin{Bmatrix} \mathbf{F_C}(t) \\ \boldsymbol{\tau}_\mathbf{C}(t) \end{Bmatrix}, \tag{2.67}$$

obeys *control laws* involving functions of either the actual state vector, or its estimation from the measurements of an output vector. We will address the derivation of control laws in later chapters. Examples of control inputs are thrust-vectoring and aerodynamic control forces and moments for aircraft and rockets, and orbital and attitude thruster force and moment, gyroscopic moment, and magnetic torques for spacecraft.

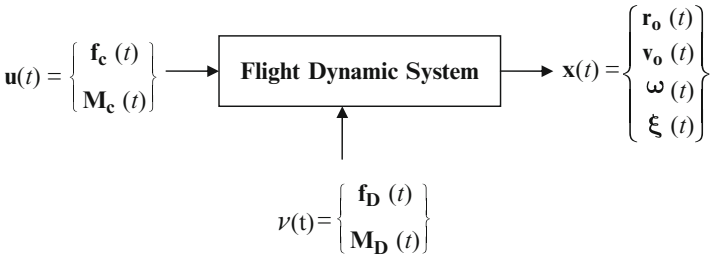

Fig. 2.5 A typical flight dynamic system

The generic flight dynamic system is depicted as a block-diagram in Fig. 2.5. Note that the environmental effects are inherent to the system, and hence are not shown as explicit inputs. Furthermore, the control laws, actuators and sensors, are excluded from Fig. 2.5. We can now express the equations governing flight dynamics as the following *state equation* to be satisfied by the state vector:

$$\frac{\mathrm{d}\boldsymbol{\zeta}}{\mathrm{d}t} = \mathbf{f}(\boldsymbol{\zeta}, \mathbf{u}, \boldsymbol{\nu}, t), \tag{2.68}$$

where $\mathbf{f}(.)$ is a vector functional possessing continuous derivatives of the state, control, and process noise vectors. The general flight dynamic system state equation is nonlinear in nature, requiring numerical methods for solution. Automatic control law derivation is generally based upon a deterministic plant, for which the noise vector vanishes, $\boldsymbol{\nu}(t) = \mathbf{0}$.

The output vector, $\mathbf{y}(t)$, of the flight dynamics system can be described by the following *output equation*:

$$\mathbf{y} = \mathbf{h}(\boldsymbol{\zeta}, \mathbf{u}, \mathbf{w}, t), \tag{2.69}$$

where $\mathbf{h}(.)$ is a vector functional and $\mathbf{w}(t)$ is a stochastic input called the *measurement noise* arising because of the imperfections in the sensors.

In advanced flight control applications called *terminal control*, (2.68) is solved iteratively in order to determine the control input, $\mathbf{u}(t)$, that drives the system's state from an initial state, $\boldsymbol{\zeta}(0)$, to a final state, $\boldsymbol{\zeta}(t_\mathrm{f})$, in a specified time, t_f. Such a mathematical problem is termed *two-point boundary value problem* (2PBVP) and requires a sophisticated solution procedure. Examples of nonlinear 2PBVP include long-range guidance of missiles and interplanetary spacecraft and are beyond our present scope. However, we shall consider some linear 2PBVP problems later.

As discussed in Chap. 1, another class of automatic flight control problems – called *tracking control* – involves tracking a known solution of the nonlinear state equation. In such cases, (2.68) is linearized about a *nominal trajectory*, $\boldsymbol{\zeta}_\mathbf{n}(t)$, that is the solution of the *unforced* state equation of the plant.

$$\frac{\mathrm{d}\boldsymbol{\zeta}_\mathbf{n}}{\mathrm{d}t} = \mathbf{f}(\boldsymbol{\zeta}_\mathbf{n}, \mathbf{0}, \mathbf{0}, t). \tag{2.70}$$

Clearly, the nominal trajectory does not require any control inputs as it is free of disturbances. When a small disturbance vector, $\boldsymbol{\nu}(t)$, is present the system requires a nonzero control input, $\mathbf{u}(t)$, to maintain the disturbed system close to the nominal trajectory. Therefore, for all intents and purposes of control law derivation, the deterministic flight dynamics plant is rendered linear by a Taylor's series expansion of (2.68) about the nominal trajectory, and the linearized state equation for deviation from the nominal trajectory, $\mathbf{x}(t) = \boldsymbol{\zeta}(t) - \boldsymbol{\zeta}_{\mathbf{n}}(t)$, is the following:

$$\frac{\mathrm{d}\mathbf{x}}{\mathrm{d}t} = \mathsf{A}(t)\mathbf{x}(t) + \mathsf{B}(t)\mathbf{u}(t), \tag{2.71}$$

where $\mathsf{A}(t), \mathsf{B}(t)$ are coefficient matrices. We will now consider some important flight dynamic systems.

2.6 Space Flight Dynamics

The generic flight dynamics system, (2.60)–(2.63), yields the following equations for space flight in the ideal vacuum environment, ($\mathbf{F_D} = \boldsymbol{\tau}_{\mathbf{E}} = \boldsymbol{\tau}_{\mathbf{D}} = \mathbf{0}$), with $\mathbf{F_E} = m\mathbf{g}$, an inertial frame of reference for translational flight and a body-fixed frame for attitude dynamics:

$$\mathbf{v} = \tfrac{\mathrm{d}\mathbf{r}}{\mathrm{d}t} = \dot{\mathbf{r}}. \tag{2.72}$$

$$\mathbf{F_C} + m\mathbf{g} = m\tfrac{\mathrm{d}\mathbf{v}}{\mathrm{d}t} = m\ddot{\mathbf{r}}. \tag{2.73}$$

$$\boldsymbol{\tau}_{\mathbf{C}} = \mathsf{J}\dot{\boldsymbol{\omega}} + \mathsf{S}(\boldsymbol{\omega})\mathsf{J}\boldsymbol{\omega}. \tag{2.74}$$

$$\dot{\mathsf{C}} = -\mathsf{S}(\boldsymbol{\omega})\mathsf{C}. \tag{2.75}$$

The space flight translational dynamics equations have unforced ($\mathbf{F_C} = \mathbf{0}$) solutions called *two-body orbits*, and the corresponding unforced rotational states ($\boldsymbol{\tau}_{\mathbf{C}} = \mathbf{0}$) are referred to as the *torque-free rotation*. Here, we shall consider the unforced trajectories that can be regarded as nominal for designing a flight control system in the presence of disturbances.

2.6.1 Orbital Mechanics

Uncontrolled flight of a spacecraft is primarily influenced by the gravity of a massive celestial object such as the Earth or the Sun, approximated to be spherical in shape and mass distribution. The gravitational perturbation due to actual, nonspherical shapes, the gravity of other distant bodies, as well as atmospheric and solar radiation effects are generally quite small in comparison with the spherical gravity of the primary body, and thus are treated as small disturbances. These disturbances are

usually compensated for by a tracking system designed around unforced, nominal trajectories (*orbits*), which are determined by the solution of the problem of two spherical bodies in mutual gravitational attraction, called the *two-body problem*. The translational dynamics equation, (2.73), can be expressed as follows for a spacecraft of mass m under the gravitational attraction of a large spherical body of mass M (called *planet*) by Newton's law of gravitation:

$$\ddot{\mathbf{r}} + \frac{\mu}{r^3}\mathbf{r} = \mathbf{0}, \tag{2.76}$$

where $\mathbf{r}(t)$ is the position of the spacecraft's center of mass relative to the planetary center and $\mu = GM$, the gravitational constant. As the planet is largely unaffected by the small spacecraft mass, the origin of the inertial frame can be taken to coincide with the planetary center that is approximated to be at rest. In order to determine the shape of an orbit, we take the vector product of both the sides of (2.76) with $\mathbf{r}$, resulting in

$$\frac{\mathrm{d}}{\mathrm{d}t}(\mathbf{r} \times \dot{\mathbf{r}}) = \mathbf{0}, \tag{2.77}$$

which implies that the *specific orbital angular momentum*,

$$\mathbf{h} = \mathbf{r} \times \dot{\mathbf{r}} = \mathbf{r} \times \mathbf{v}, \tag{2.78}$$

is conserved. Because $\mathbf{h}$ is a constant vector, it follows that:

(a) The direction of $\mathbf{h}$ is a constant, which implies that the vectors $\mathbf{r}$ and $\mathbf{v}$ are always in the same plane – called *orbital plane* – and $\mathbf{h}$ is normal to that plane.
(b) The magnitude of $\mathbf{h}$ is constant. Writing $\mathbf{h}$ in polar coordinates, (r, θ),

$$h = |\ \mathbf{h}\ | = |\ \mathbf{r} \times \mathbf{v}\ | = r^2\dot{\theta}, \tag{2.79}$$

this implies that the radius vector, $\mathbf{r}$, sweeps out area at a constant rate, $\frac{1}{2}r^2\dot{\theta}$ (Kepler's second law of planetary motion).

The orbits are classified according to the magnitude and direction of the constant angular momentum, $\mathbf{h}$.

By taking the vector product of both sides of (2.76) with $\mathbf{h}$, it can be shown that the following *eccentricity vector*, $\mathbf{e}$, is a constant:

$$\mathbf{e} = \frac{1}{\mu}(\mathbf{v} \times \mathbf{h}) - \frac{\mathbf{r}}{r}. \tag{2.80}$$

As the eccentricity vector is normal to $\mathbf{h}$, it lies in the orbital plane and can be used as a reference for the direction of the position vector, $\mathbf{r}(t)$. The angle, $\theta(t)$, made by $\mathbf{r}(t)$ with $\mathbf{e}$ (measured along the flight direction) is called the *true anomaly*.

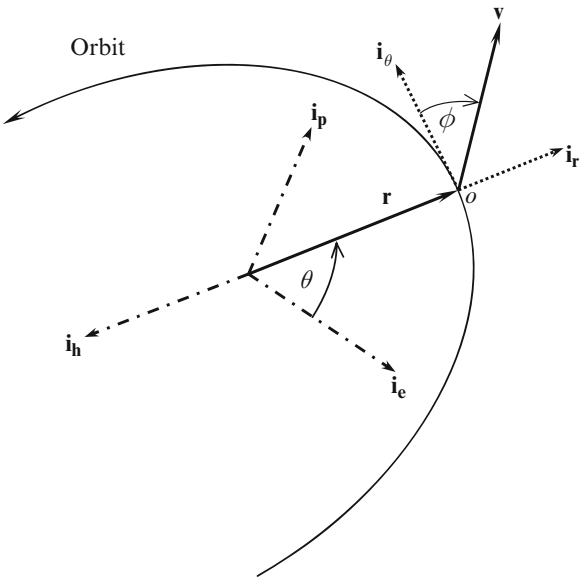

Fig. 2.6 Spacecraft's orbital position and velocity resolved in the perifocal frame, $\mathbf{i_e}, \mathbf{i_p}, \mathbf{i_h}$

Figure 2.6 depicts an orbital coordinate system consisting of unit vectors, $\mathbf{i_e}, \mathbf{i_h}$ along $\mathbf{e}, \mathbf{h}$, respectively, and a third unit vector, $\mathbf{i_p}$, normal to both $\mathbf{e}$ and $\mathbf{h}$ such that

$$\mathbf{i_h} = \mathbf{i_e} \times \mathbf{i_p}. \tag{2.81}$$

Such a coordinate system, called the *perifocal frame*, is useful in resolving the position vector in the orbital plane in terms of the true anomaly, $\theta(t)$:

$$\mathbf{r} = r\left(\mathbf{i_e}\cos\theta + \mathbf{i_p}\sin\theta\right). \tag{2.82}$$

As the velocity vector always lies in the orbital plane, $(\mathbf{i_e}, \mathbf{i_p})$, one can express the velocity in terms of the flight path angle, ϕ, as follows (Fig. 2.6):

$$\mathbf{v} = v\left[\sin(\phi-\theta)\mathbf{i_e} + \cos(\phi-\theta)\mathbf{i_p}\right]. \tag{2.83}$$

By substituting (2.82) and (2.83) into (2.78), we have

$$h = rv\cos\phi. \tag{2.84}$$

By taking the scalar product of $\mathbf{e}$ with $\mathbf{r}(t)$ we have

$$r + \mathbf{e}\cdot\mathbf{r} = \frac{1}{\mu}\mathbf{r}\cdot(\mathbf{v}\times\mathbf{h}) = \frac{h^2}{\mu}, \tag{2.85}$$

or,

$$r = \frac{h^2/\mu}{1 + e\cos\theta}. \tag{2.86}$$

Equation (2.86) – called the *orbit equation* – defines the shape of the orbit in polar coordinates, (r, θ), and indicates that the orbit is symmetrical about $\mathbf{i_e}$. Furthermore, the minimum separation of the two bodies (called *periapsis*) occurs for $\theta = 0$, implying that $\mathbf{i_e}$ points toward the periapsis. From the orbit equation it is clear that the general orbit is a *conic section*, i.e., the shape one gets by cutting a right-circular cone in a given way. For $e < 1$, the orbit is an *ellipse*. The circle is a special ellipse with $e = 0$ and $r = h^2/\mu$. For $e = 1$, the orbit is a *parabola*. The *rectilinear* trajectory is a special parabola with $h = 0$. For $e > 1$, the orbit is a *hyperbola*. In all cases, the *focus* of the orbit is at the center of the celestial body, and the *semimajor axis*, a, is given by:

$$a = \frac{h^2/\mu}{1 - e^2}. \tag{2.87}$$

Another useful orbital constant is the parameter, p, defined as the radius when $\theta = \pi/2$:

$$p = r|_{\theta=\pi/2} = h^2/\mu = a(1 - e^2), \tag{2.88}$$

which enables the orbit equation to be written as follows:

$$r = \frac{p}{1 + e\cos\theta}. \tag{2.89}$$

By substituting the orbit equation into (2.84), we have

$$\cos\phi = \frac{\mu(1 + e\cos\theta)}{hv}. \tag{2.90}$$

By taking the time derivative of the orbit equation and equating it to the radial velocity component, $\dot{r} = v\sin\phi$ (Fig. 2.6), we write

$$\dot{r} = v\sin\phi = \frac{ep\sin\theta}{1 + e\cos\theta}\dot{\theta}, \tag{2.91}$$

which by substitution of (2.79), becomes

$$\sin\phi = \frac{\mu e\sin\theta}{hv}. \tag{2.92}$$

Equations (2.90) and (2.92) allow us to determine the flight path angle, ϕ, uniquely from the true anomaly, θ. On eliminating the flight path angle from the velocity expression, (2.83), results in the following simplification:

$$\mathbf{v} = \frac{\mu}{h}\left[-\sin\theta\mathbf{i_e} + (e + \cos\theta)\mathbf{i_p}\right]. \tag{2.93}$$

2.6.1.1 Kepler's Equation

The vectors **h** and **e** completely determine the shape and orientation of a two-body trajectory, but do not provide any information about the location of the spacecraft at a given time. This missing data is usually expressed as an equation that relates the variation of true anomaly with time, $\theta(t)$, beginning with the *time of periapsis*, τ, for which $\theta = 0$. On substituting the orbit equation, (2.89), into (2.79), we have

$$\dot{\theta} = \sqrt{\frac{\mu}{p^3}}(1 + e\cos\theta)^2. \tag{2.94}$$

The time integral of (2.94) provides τ, thereby determining the function $\theta(t)$, and completing the solution to the two-body problem. However, because of the nonlinear nature of (2.94), such an integration is usually carried out by a numerical procedure. For illustration, we will consider only the elliptical orbit and refer the reader to Tewari [21] for other details.

For an elliptical orbit ($0 < e < 1$), (2.94) becomes

$$\frac{(1-e^2)^{\frac{3}{2}}\mathrm{d}\theta}{(1+e\cos\theta)^2} = n\mathrm{d}t, \tag{2.95}$$

where

$$n \doteq \sqrt{\frac{\mu}{a^3}} \tag{2.96}$$

is referred to as the orbital *mean motion*. In order to simplify (2.95), we introduce an *eccentric anomaly, E* defined by:

$$\cos E = \frac{e + \cos\theta}{1 + e\cos\theta} \tag{2.97}$$

which substituted into (2.95) yields the following *Kepler's equation*:

$$E - e\sin E = M, \tag{2.98}$$

where $M = n(t - \tau)$ is called the *mean anomaly*. The relationship between the true and the eccentric anomalies is given by the following:

$$\tan\frac{\theta}{2} = \sqrt{\frac{1+e}{1-e}}\tan\frac{E}{2}. \tag{2.99}$$

Note that $E/2$ and $\theta/2$ are always in the same quadrant. A numerical solution to Kepler's equation can be easily obtained by Newton–Raphson's method [21].

Given the position and velocity at some time, t_0, one would often like to determine the position and velocity at some other time, t, which translates into determining eccentric anomaly, E, from a given mean anomaly, M. After solving Kepler's equation for E, we can express the position and velocity vectors of an elliptical orbit directly as follows:

$$\begin{aligned}\mathbf{r} &= a(\cos E - e)\mathbf{i_e} + \sqrt{ap}\sin E\mathbf{i_p}\\ \mathbf{v} &= -\frac{\sqrt{\mu a}}{r}\sin E\mathbf{i_e} + \frac{\sqrt{\mu p}}{r}\cos E\mathbf{i_p}.\end{aligned} \tag{2.100}$$

2.6.1.2 Celestial Frame of Reference

The spacecraft's position and velocity are generally resolved in an inertial, *celestial frame*, $(\mathbf{I}, \mathbf{J}, \mathbf{K})$, which is fixed with respect to distant stars and has its origin at the center of the celestial body. An example of celestial frames is the *equatorial frame* of Earth, with the axis $\mathbf{I}$ pointing in the direction of *vernal equinox* – the unique point of the Sun's apparent annual crossing of the equatorial plane from the south to the north. The other two axes of the frame are chosen such that $\mathbf{K}$ is the polar axis, and $\mathbf{I}\times\mathbf{J} = \mathbf{K}$, as shown in Fig. 2.7. The orientation of the right-handed perifocal, orbital frame, $\mathbf{i_e}, \mathbf{i_p}, \mathbf{i_h}$, relative to the celestial frame, $(\mathbf{I}, \mathbf{J}, \mathbf{K})$, is classically represented by the Euler angles sequence, $(\Omega)_3, (i)_1, (\omega)_3$, as shown in Fig. 2.7. However, such a representation has singularities at $i = 0, \pi$, as we know from earlier discussion.

The intersection of the spacecraft's orbital plane with the equatorial plane yields the *line of nodes*. The *ascending node* is the name given to the point on the line of nodes where the orbit crosses the equatorial plane from the south to the north, as shown in Fig. 2.7. The unit nodal vector, $\mathbf{n}$, pointing toward the ascending node makes an angle Ω with the axis $\mathbf{I}$, measured in the equatorial plane in an anticlockwise direction (Fig. 2.7). The angle Ω is termed *right ascension of the ascending node*. The *orbital inclination*, i, is the angle made by the orbital plane with the equatorial plane, and is also the positive rotation about $\mathbf{n}$ required to produce $\mathbf{i_h}$ from the axis $\mathbf{K}$. The third Euler angle ω represents a positive rotation of $\mathbf{n}$ about $\mathbf{i_h}$ to produce $\mathbf{i_e}$ in the orbital plane, and is called *argument of periapsis*.

The coordinate transformation between the perifocal and the celestial frames is given by the following rotation matrix:

$$\mathsf{C} = \mathsf{C}_3(\omega)\mathsf{C}_1(i)\mathsf{C}_3(\Omega), \tag{2.101}$$

where

$$\begin{Bmatrix}\mathbf{I}\\ \mathbf{J}\\ \mathbf{K}\end{Bmatrix} = \mathsf{C}^{\mathrm{T}}\begin{Bmatrix}\mathbf{i_e}\\ \mathbf{i_p}\\ \mathbf{i_h}\end{Bmatrix}. \tag{2.102}$$

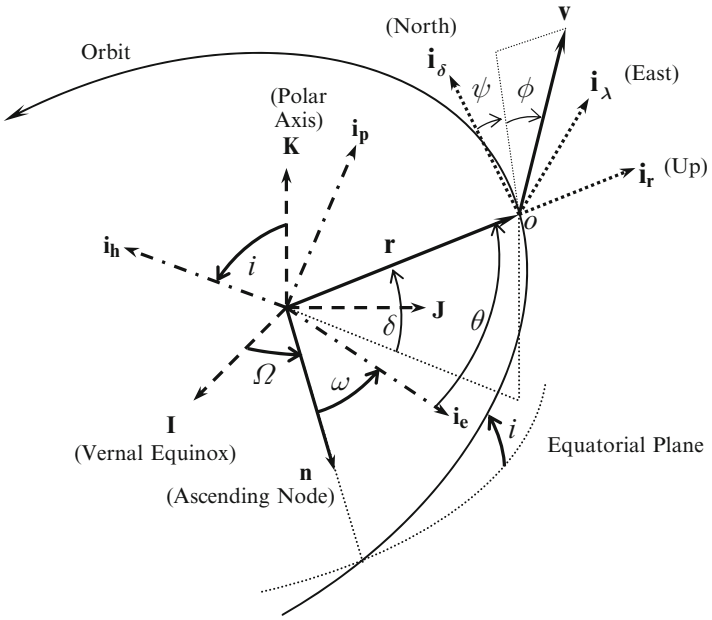

Fig. 2.7 Spacecraft's orbital geometry: (**a**) orientation of the perifocal frame, $\mathbf{i_e}, \mathbf{i_p}, \mathbf{i_h}$, relative to celestial plane, $(\mathbf{I}, \mathbf{J}, \mathbf{K})$, given by Euler angles, $(\Omega)_3, (i)_1, (\omega)_3$, (**b**) the orbital velocity vector resolved in the local horizon frame, $(\mathbf{i_r}, \mathbf{i_\lambda}, \mathbf{i_\delta})$

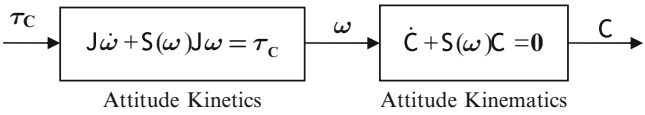

Fig. 2.8 Spacecraft's attitude plant subsystems in a cascade relationship

2.6.2 *Spacecraft Attitude Dynamics*

In contrast with atmospheric flight mechanics, there is no coupling between the attitudinal (rotational) and the translational motions of a spacecraft. This fact offers a great simplification, in which a cascade relationship is possible between rotational kinetics (2.74) and rotational kinematics (2.75). Such a relationship is depicted in Fig. 2.8, where we see that the control torque, $\boldsymbol{\tau}_\mathbf{C}(t)$, is the applied input to the rotational kinetics block whose output, $\boldsymbol{\omega}(t)$, serves as the input to the rotational kinematics subsystem. Hence, one can separately design control laws for the two subsystems. The control torque is applied either externally by rocket thrusters or internally by rotors (reaction wheels and gyros). We shall return to spacecraft attitude control in Chap. 6.

2.7 Atmospheric Flight Dynamics

Atmospheric flight is dominated by aerodynamic forces and moments. The linear velocity of the rigid flight vehicle's center of mass, $\mathbf{v}$, and the angular velocity about the center of mass, $\boldsymbol{\omega}$, both relative to a reference frame, $(\mathbf{I}, \mathbf{J}, \mathbf{K})$, are resolved in a body-fixed frame, $(\mathbf{i}, \mathbf{j}, \mathbf{k})$, (Fig. 2.9) with origin at the center of mass as follows:

$$\mathbf{v} = U\mathbf{i} + V\mathbf{j} + W\mathbf{k}, \tag{2.103}$$

and

$$\boldsymbol{\omega} = P\mathbf{i} + Q\mathbf{j} + R\mathbf{k}. \tag{2.104}$$

Borrowing from aeronautical terminology, U is called the *forward speed*, V the *sideslip speed*, and W the *plunge* (or *downward*) *speed*. Furthermore, P is called the *roll rate*, Q the *pitch rate*, and R the *yaw rate*. The aerodynamic moment, $\boldsymbol{\tau}_{\mathbf{a}}$, is resolved in the body-fixed frame, $(oxyz)$ as follows:

$$\boldsymbol{\tau}_{\mathbf{a}} = L\mathbf{i} + M\mathbf{j} + N\mathbf{k}, \tag{2.105}$$

where L is called the *rolling moment*, M the *pitching moment*, and N is the *yawing moment*. The engine thrust, $\mathbf{T}(t)$, resolved in the body-fixed frame using *thrust angles*, $\mu_1(t)$, $\mu_2(t)$, (Fig. 2.10) is the following:

$$\mathbf{T} = T(\mathbf{i}\cos\mu_1\cos\mu_2 + \mathbf{j}\cos\mu_1\sin\mu_2 + \mathbf{k}\sin\mu_1). \tag{2.106}$$

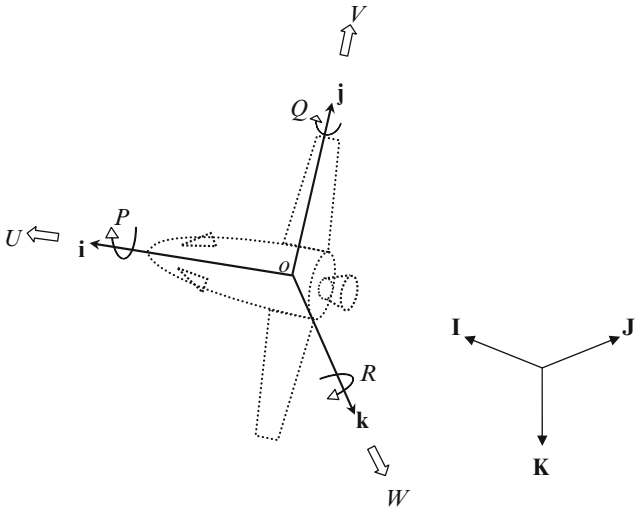

Fig. 2.9 A body-fixed frame, $(\mathbf{i}, \mathbf{j}, \mathbf{k})$, relative to a reference frame, $(\mathbf{I}, \mathbf{J}, \mathbf{K})$

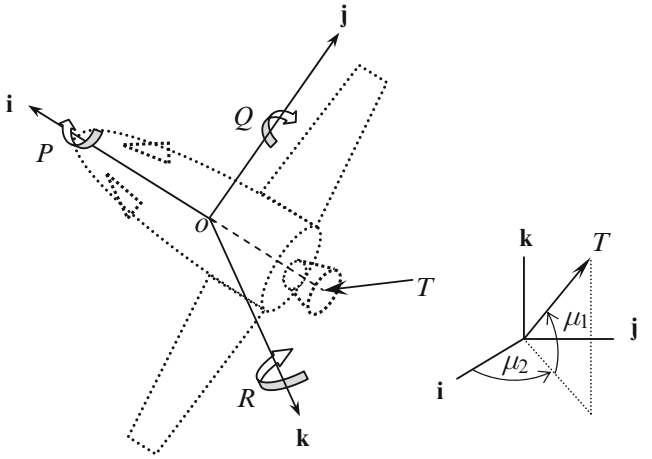

Fig. 2.10 The body-fixed frame, $(\mathbf{i}, \mathbf{j}, \mathbf{k})$, and thrust angles, ϵ and γ

Propulsive efficiency requires that the thrust angles should be small, which results in the approximation

$$\mathbf{T} \simeq T(\mathbf{i} + \mathbf{j}\mu_2 + \mathbf{k}\mu_1). \tag{2.107}$$

Furthermore, the control torque applied by thrust deflection is the following:

For aircraft stability and control applications (Chap. 4), the thrust is usually clubbed with the aerodynamic force vector, $\mathbf{F_a}$, as follows:

$$\mathbf{F_a} + \mathbf{T} = X\mathbf{i} + Y\mathbf{j} + Z\mathbf{k}, \tag{2.108}$$

where X is called the *forward force*, Y the *sideforce*, and Z is the *downward force*.

The general attitude kinematics of an atmospheric flight vehicle can be represented by the quaternion, (q_1, q_2, q_3, q_4). Of the translational kinematic variables, only the altitude, h, is important as it governs the atmospheric properties and thus aerodynamic forces and moments. Therefore, we generally have a seven degree-of-freedom, eleventh-order, basic flight dynamics model shown in Fig. 2.11. However, when applied to the level flight dynamics of aircraft (Chap. 4), the variation in altitude for stability and control applications is negligible, and the quaternion is typically replaced by the Euler angles, resulting in a six degree-of-freedom, ninth-order system.

2.7.1 Wind Axes

It is often difficult to express the aerodynamic forces directly in the body-fixed frame, for which another moving reference frame with an axis, $\mathbf{i_v}$, along the

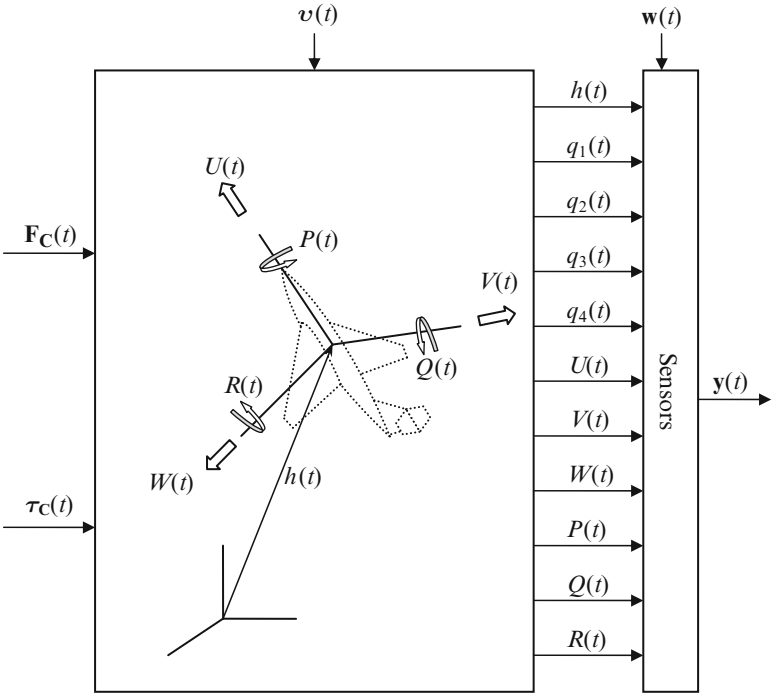

Fig. 2.11 Atmospheric flight dynamics system

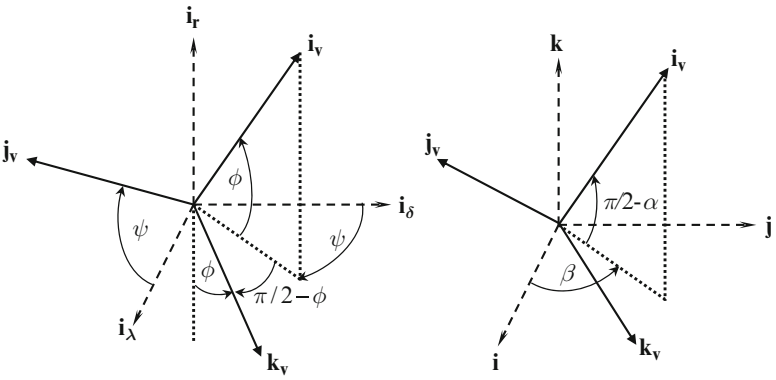

Fig. 2.12 The wind axes, $(\mathbf{i_v}, \mathbf{j_v}, \mathbf{k_v})$, relative to the body-fixed frame, $(\mathbf{i}, \mathbf{j}, \mathbf{k})$, and the local horizon frame, $(\mathbf{i_r}, \mathbf{i_\lambda}, \mathbf{i_\delta})$

instantaneous relative velocity vector, $\mathbf{v}(t)$, is chosen for convenience. Such a frame, $ox_vy_vz_v$, called *wind axes*, is shown in Fig. 2.12 and is very useful in expressing the aerodynamic force, $\mathbf{F_a}$, and aerodynamic moment, $\boldsymbol{\tau}_\mathbf{a}$, both of which, by definition,

depend upon the relative motion between the vehicle and the atmosphere.[3] The *lift*, $\mathcal{L}$, the *driftforce*, f_y, and the *drag*, $\mathcal{D}$ are the components of the aerodynamic force vector along the wind axes:

$$\mathbf{F_a} = -\mathcal{D}\mathbf{i_v} + f_y\mathbf{j_v} - \mathcal{L}\mathbf{k_v}. \tag{2.109}$$

Note that the lift and driftforce act normal to the flight direction, $\mathbf{i_v}$, thereby causing a change of flight path, while drag is always opposed to it and acts as an energy sink.

The coordinate transformation between the wind axes and the local horizon frame is given by the Euler angle sequence $(-\psi)_1, (\phi - \frac{\pi}{2})_2$:

$$\left\{\begin{array}{c}\mathbf{i_v}\\ \mathbf{j_v}\\ \mathbf{k_v}\end{array}\right\} = \mathsf{C}_W \left\{\begin{array}{c}\mathbf{i_r}\\ \mathbf{i_\lambda}\\ \mathbf{i_{ffi}}\end{array}\right\}, \tag{2.110}$$

where

$$\mathsf{C}_W = \mathsf{C}_2\left(\phi - \frac{\pi}{2}\right)\mathsf{C}_1(-\psi) = \begin{pmatrix}\sin\phi & \cos\phi\sin\psi & \cos\phi\cos\psi\\ 0 & \cos\psi & -\sin\psi\\ -\cos\phi & \sin\phi\sin\psi & \sin\phi\cos\psi\end{pmatrix} \tag{2.111}$$

The linear acceleration of the vehicle's center of mass can be expressed in the wind axes as follows:

$$\dot{\mathbf{v}} = a_{xv}\mathbf{i_v} + a_{yv}\mathbf{j_v} + a_{zv}\mathbf{k_v}, \tag{2.112}$$

where

$$\begin{aligned} a_{xv} &= \dot{v} + \Omega^2 r\cos\delta(\cos\phi\cos\psi\sin\delta - \sin\phi\cos\delta)\\ a_{yv} &= v\cos\phi\dot{\psi} - \frac{v^2}{r}\cos^2\phi\sin\psi\tan\delta - \Omega^2 r\sin\psi\sin\delta\cos\delta\\ &\quad +2\Omega v(\sin\phi\cos\psi\cos\delta - \cos\phi\sin\delta)\\ a_{zv} &= -v\dot{\phi} + \frac{v^2}{r}\cos\phi + 2\Omega v\sin\psi\cos\delta\\ &\quad +\Omega^2 r\cos\delta(\sin\phi\cos\psi\sin\delta + \cos\phi\cos\delta). \end{aligned} \tag{2.113}$$

In stability and control applications, the planetary rotation is typically neglected, leading to a simplification in the acceleration terms.

[3] Even when the aerodynamics is unimportant (as in space flight), the wind axes provide a convenient reference frame for the vehicle's attitude.

For aerodynamic purposes, the orientation of the body-fixed frame, $(oxyz)$, relative to the wind axes is given by the Euler angles, α (*angle-of-attack*) and β (*sideslip angle*) in the sequence $(\beta)_3, (-\alpha)_2$ (Fig. 2.12). The coordinate transformation between the wind axes and the body-fixed frame is thus given by:

$$\begin{Bmatrix} \mathbf{i_v} \\ \mathbf{j_v} \\ \mathbf{k_v} \end{Bmatrix} = \mathsf{C}_B \begin{Bmatrix} \mathbf{i} \\ \mathbf{j} \\ \mathbf{k} \end{Bmatrix}, \tag{2.114}$$

where

$$\mathsf{C}_B = \begin{pmatrix} \cos\alpha\cos\beta & \cos\alpha\sin\beta & \sin\alpha \\ -\sin\beta & \cos\beta & 0 \\ -\sin\alpha\cos\beta & -\sin\alpha\sin\beta & \cos\alpha \end{pmatrix} \tag{2.115}$$

Referring to Fig. 2.12 and the first row of (2.114) we write

$$\mathbf{v} = v(\cos\alpha\cos\beta\mathbf{i} + \cos\alpha\sin\beta\mathbf{j} + \sin\alpha\mathbf{k}), \tag{2.116}$$

where the angle-of-attack and the sideslip angle are related to the relative velocity components as follows:

$$\alpha = \sin^{-1}\frac{W}{\sqrt{U^2+V^2+W^2}}, \tag{2.117}$$

$$\beta = \tan^{-1}\frac{V}{U}. \tag{2.118}$$

The dependence of the aerodynamic forces on the angle-of-attack and the sideslip angle is crucial to stability and control.

2.7.2 Aerodynamic Forces and Moments

The fundamental sources of aerodynamic forces and moments are the surface distributions of static pressure, $p(x, y, z, t)$, acting normal to the surface, and shear stress, $\tau(x, y, z, t)$, along the relative flow direction. When integrated over the entire exposed surface of the vehicle, the pressure and shear stress distributions give rise to the aerodynamic force vector, $\mathbf{F_a}(t)$, and aerodynamic torque vector, $\boldsymbol{\tau}_a(t)$, as functions of the relative flow velocity far upstream, (v, α, β), called the *freestream velocity*, the linear flow acceleration, $(\dot{v}, \dot{\alpha}, \dot{\beta})$, the angular velocity of the vehicle, (P, Q, R), as well as thermodynamic properties of the freestream, namely density, ρ, static temperature, $\bar{T}$, dynamic viscosity, $\bar{\mu}$, and specific-heat ratio, γ. When the flow does not have any intermolecular voids, it is regarded to be a continuum governed by nondimensional parameters such as the *Mach number*, $\mathcal{M} = v/a$, where a is the speed of sound far upstream, and the *Reynolds number*, $Re = (\rho v\ell)/\bar{\mu}$, with ℓ being a characteristic length of the flow. When

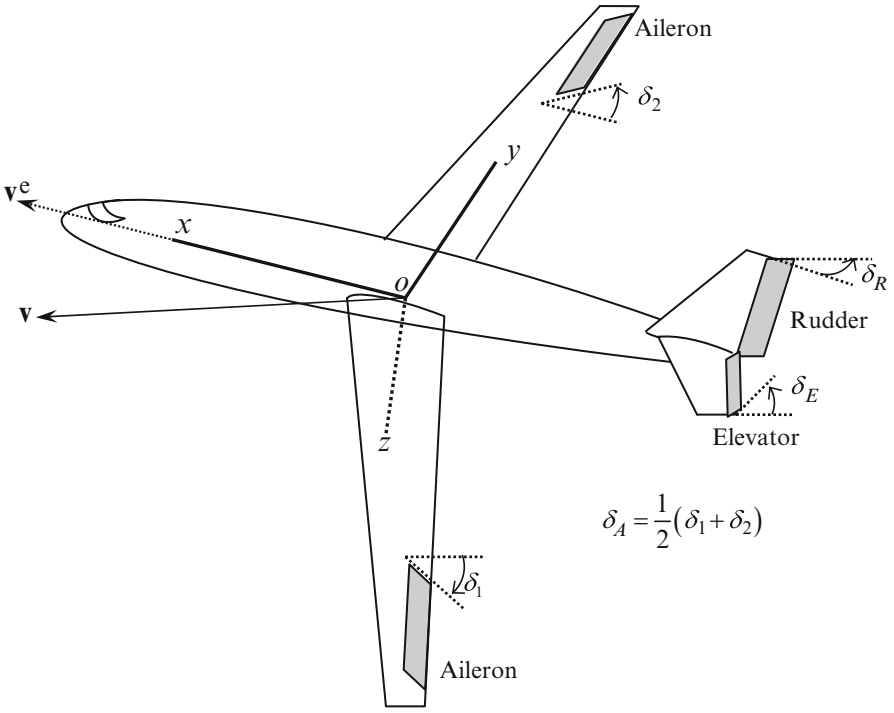

Fig. 2.13 The stability axes, $(oxyz)$, and the aerodynamic control surfaces

the characteristic length becomes either comparable to or larger than the *mean free-path*, $\bar{\lambda}$, of the gas molecules, we have a rarefied flow in which the governing flow parameter is *Knudsen number* given by $Kn = \bar{\lambda}/\ell$. Based upon Knudsen number, the flow regimes are commonly classified as (a) *Free-molecular* flow, $(Kn \geq 10)$, (b) *Transition flow* flow, $(0.01 \leq Kn \leq 10)$, (c) *Continuum* flow, $(Kn \leq 0.01)$.

2.7.2.1 Stability Axes, Small Perturbations, and Control Surfaces

When the nominal trajectory is a steady maneuver, the aerodynamic force and torque are balanced by other effects, and thus have constant equilibrium values, $\mathbf{F_a}^e, \boldsymbol{\tau}^e_{\mathbf{a}}$. In such a case, a special body-fixed frame – called *stability axes* – is generally employed having one axis initially aligned with the nominal flight direction (Fig. 2.13). Furthermore, as all atmospheric flight vehicles have at least one plane of symmetry, (oxz), the equilibrium velocity vector lies in the plane of symmetry and we have

$$\alpha^e = 0$$

$$\beta^e = 0,$$

or, $\mathbf{v}^e = U^e\mathbf{i}$.

A small perturbation, $\Delta\mathbf{v}(t), \Delta\boldsymbol{\omega}(t)$, that begins acting at $t = 0$ about the equilibrium point, $\mathbf{v}^{\mathrm{e}}, \boldsymbol{\omega}^{\mathrm{e}}$, causes small changes in the flow speed, $u(t)$, angle-of-attack, $\alpha(t)$, sideslip angle, $\beta(t)$, and body-rates, $p(t), q(t), r(t)$, measured with respect to the stability axes:

$$\begin{aligned} \mathbf{v} &= \mathbf{v}^{\mathrm{e}} + \Delta\mathbf{v} \\ \boldsymbol{\omega} &= \boldsymbol{\omega}^{\mathrm{e}} + \Delta\boldsymbol{\omega}, \end{aligned} \tag{2.119}$$

or,

$$\begin{aligned} U &= U^{\mathrm{e}} + u \\ V &= U^{\mathrm{e}}\beta \\ W &= U^{\mathrm{e}}\alpha \\ P &= P^{\mathrm{e}} + p \\ Q &= Q^{\mathrm{e}} + q \\ R &= R^{\mathrm{e}} + r. \end{aligned}$$

As mentioned earlier, the aerodynamic force and torque depend not only upon the linear and angular velocity perturbations, $u, \alpha, \beta, p, q, r$, but also on the linear acceleration perturbations, $\dot{u}, \dot{\alpha}, \dot{\beta}$, due to unsteady flow. These latter perturbations cause a delay (or lag) in the onset of aerodynamic changes and are thus termed *aerodynamic inertia* effects.

The aerodynamic force and torque are controlled by small deflections of control surfaces. Generally, the aerodynamic forces and moments obey linear relationships with control surface deflections. Furthermore, the control surfaces are driven by actuators with a dynamic response about ten times faster than that of the vehicle's rigid body dynamics. Therefore, flow unsteadiness due to control surface deflections can often be neglected when considering rigid body aerodynamics. Hence, a quasi-steady approximation of aerodynamic loads, linearly varying with control surface deflection, is usually employed.[4]

The aerodynamic control surface for longitudinal control is the *elevator* with rotation axis parallel to oy (Fig. 2.13). The elevator can be mounted either forward or behind oy, usually on the trailing edge of a larger stabilizing surface in the oxy plane, as shown in Fig. 2.13. Elevator deflection, δ_{E}, creates a forward force, $X_{\delta}\delta_{\mathrm{E}}$, downforce, $Z_{\delta}\delta_{\mathrm{E}}$, and a control pitching moment, $M_{\delta}\delta_{\mathrm{E}}$.

A pair of control surfaces in the oxy plane, located symmetrically about the axis ox and deflected in mutually opposite directions by angles δ_1 and δ_2 (Fig. 2.13) are

[4]When the vehicle's structural flexibility is taken into account, it is necessary to include the unsteady aerodynamic effects of control surface deflections, i.e., dependence of aerodynamic forces and moments on deflection rates, $\dot{\delta}_{\mathrm{E}}, \dot{\delta}_{\mathrm{A}}, \dot{\delta}_{\mathrm{R}}$.

called *ailerons* that are used as roll control devices. The *aileron deflection* is the average of the two separate deflections, $\delta_{\mathrm{A}} = (\delta_1 + \delta_2)/2$, and is designed such that a control rolling moment, $L_{\mathrm{A}}\delta_{\mathrm{A}}$, is produced along with a much smaller, undesirable yawing moment, $N_{\mathrm{A}}\delta_{\mathrm{A}}$, called adverse aileron yaw. A control surface mounted on a fin in the oxz plane behind the oy axis is called the *rudder*, and is shown in Fig. 2.13. A rudder deflection, δ_{R}, creates a sideforce, $Y_{\mathrm{R}}\delta_{\mathrm{R}}$, control yawing moment, $N_{\mathrm{R}}\delta_{\mathrm{R}}$, and a much smaller rolling moment, $L_{\mathrm{R}}\delta_{\mathrm{R}}$. Rudder is primarily used to correct a lateral flight asymmetry. For a rocket's flight through the atmosphere, the control surfaces consist of movable fins that can exert rolling, pitching, and yawing moments by simultaneous deflection. In addition to the aerodynamic controls, some vehicles have a thrust vectoring capability that can be used for applying control forces and moments.

We note that due to inertia coupling, rotational kinetics produces equilibrium solutions whenever any two body rates vanish for a zero net external torque. Hence, we assume that for equilibrium, only one of the body rates is nonzero, and all the aerodynamic moments are zeros. Furthermore, the aerodynamic moments in atmospheric flight are much larger than the typical internal rotor torques, which are commonly neglected in rotational dynamics. All of the assumptions in this paragraph cause the aerodynamic perturbations in the plane of symmetry oxz – called the *longitudinal plane* (or *pitch plane*) – to be decoupled from those taking place out-of-plane. Thus, the pitching moment, M, forward force, X, and downforce, Z, depend only on the longitudinal perturbations, $u, \alpha, \dot{u}, \dot{\alpha}, q$. On the other hand, the rolling moment, L, sideforce, Y, and yawing moment, N, depend only on the lateral perturbations, $\beta, \sigma, \dot{\beta}, p, r$.[5]

On expanding the aerodynamic forces and moments in a Taylor series about the equilibrium point and assuming small distubances, we have the following linear approximations:

$$\begin{aligned} X &= X^{\mathrm{e}} + X_u u + X_\alpha \alpha + X_{\dot{u}}\dot{u} + X_{\dot{\alpha}}\dot{\alpha} + X_q q + X_\delta \delta_{\mathrm{E}} \\ Z &= Z^{\mathrm{e}} + Z_u u + Z_\alpha \alpha + Z_{\dot{u}}\dot{u} + Z_{\dot{\alpha}}\dot{\alpha} + Z_q q + Z_\delta \delta_{\mathrm{E}} \\ M &= M^{\mathrm{e}} + M_u u + M_\alpha \alpha + M_{\dot{u}}\dot{u} + M_{\dot{\alpha}}\dot{\alpha} + M_q q + M_\delta \delta_{\mathrm{E}}, \end{aligned} \tag{2.120}$$

and

$$\begin{aligned} Y &= Y^{\mathrm{e}} + Y_\beta \beta + Y_\sigma \sigma + Y_{\dot{\beta}}\dot{\beta} + Y_p p + Y_r r + Y_{\mathrm{R}}\delta_{\mathrm{R}} \\ L &= L^{\mathrm{e}} + L_\beta \beta + L_\sigma \sigma + L_{\dot{\beta}}\dot{\beta} + L_p p + L_r r + L_{\mathrm{A}}\delta_{\mathrm{A}} + L_{\mathrm{R}}\delta_{\mathrm{R}} \\ N &= N^{\mathrm{e}} + N_\beta \beta + N_\sigma \sigma + N_{\dot{\beta}}\dot{\beta} + N_p p + N_r r + N_{\mathrm{A}}\delta_{\mathrm{A}} + N_{\mathrm{R}}\delta_{\mathrm{R}}, \end{aligned} \tag{2.121}$$

[5]Missiles rolling at a high rate can have a significant aerodynamic coupling between longitudinal and lateral aerodynamics. However, as such motions are inherently nonlinear, they are beyond our present scope.

where the coefficients stand for partial derivatives with respect to the subscripted variable at equilibrium, e.g.,

$$X_u = \left.\frac{\partial X}{\partial u}\right|_{u=0}. \tag{2.122}$$

The coefficients related to the motion variables, $u, \alpha, \beta, \dot{u}, \dot{\alpha}, \dot{\beta}, \sigma, p, q, r$, are called *stability derivatives* as they influence the stability of the equilibrium point, while those related to the control inputs, $\delta_{\mathrm{E}}, \delta_{\mathrm{A}}, \delta_{\mathrm{R}}$, are termed *control derivatives*.

The aerodynamic force and torque are usually nondimensionalized as follows:

$$\begin{aligned}\mathbf{F_a} &= \frac{1}{2}\rho v^2 S \mathbf{C_F}\\ \boldsymbol{\tau}_\mathbf{a} &= \frac{1}{2}\rho v^2 S \ell \mathbf{C}_{\boldsymbol{\tau}},\end{aligned} \tag{2.123}$$

where $\mathbf{C_F}, \mathbf{C}_{\boldsymbol{\tau}}$ are nondimensional force and torque coefficient vectors, respectively, whose functional dependence on the nondimensional flow variables, $\alpha, \beta, Kn, \mathcal{M}, Re$, is obtained either experimentally in a wind-tunnel or by a computational fluid dynamics (CFD) model. The external shape of the vehicle is primarily important for such nondimensional relationships. The nondimensional lift, C_{L}, drag, C_{D}, and sideforce, C_y, coefficients are the components of $\mathbf{C_F}$ resolved along the wind axes, while the rolling moment, C_ℓ, pitching moment, C_m, and yawing moment, C_n coefficients are the components of $\mathbf{C}_{\boldsymbol{\tau}}$ resolved along the body axes. As the parameters governing the flow (i.e., $v, \rho, a, Kn, \mathcal{M}, Re$) vary little in the vicinity of a given equilibrium flight condition, they are assumed constants in a stability and control analysis, which only requires small disturbances from equilibrium, as discussed earlier. Thus, for the purpose of control system design, the aerodynamic system can be modeled as a linear system.

Example 2.1. Let us revisit the aircraft level flight model presented in Example 1.3. With airspeed, $v(t)$, azimuth, $\psi(t)$, latitude, $\delta(t)$, and longitude, $\lambda(t)$, the equations of translational motion are the following:

$$\begin{aligned}\dot{\delta} &= \frac{v\cos\psi + v_{\mathrm{w}}\cos\psi_{\mathrm{w}}}{R_0 + h}\\ \dot{\lambda} &= \frac{v\sin\psi + v_{\mathrm{w}}\sin\psi_{\mathrm{w}}}{(R_0 + h)\cos\delta}\\ v\dot{\psi} &= g\tan\sigma + \frac{1}{2}\Omega^2(R_0 + h)\sin\psi\sin 2\delta - 2\Omega v\cos\psi\cos\delta\\ m\dot{v} &= T(v) + \Delta T - \frac{1}{2}\rho v^2 S\left(C_{\mathrm{D}0} + \frac{4Km^2g^2\sec^2\sigma}{\rho^2 S^2 v^4}\right)\\ &\quad -\frac{1}{2}m\Omega^2(R_0 + h)\cos\psi\sin 2\delta,\end{aligned} \tag{2.124}$$

where R_0 (Earth's radius), Ω (Earth's rotational rate), ρ (atmospheric density), S (wing area), C_{D0} (parasite drag-coefficient), K (lift-dependent drag factor), and g (acceleration due to gravity) are constants. The mass, $m(t)$, is a specified function of time. The engine thrust, $T(v)$, is a known function of speed at a constant throttle setting, while $\Delta T(t)$ is a control input applied to the aircraft by changing the throttle setting. Another control input is the bank angle, $\sigma(t)$, measured from the local horizontal plane. Both the inputs are applied by either a pilot or an automatic control system. The wind speed, $v_w(t)$, and wind azimuth, $\psi_w(t)$, are stochastic (random) inputs, regarded as disturbances. It is assumed that the angle-of-attack (and thus lift) is adjusted automatically in order to maintain level flight, and all turns are automatically coordinated by rudder input.

The thrust actuating mechanism is modeled by the following second-order differential equation:

$$a_1 \frac{d^2 \Delta T}{dt^2} + a_2 \frac{d\Delta T}{dt} + a_3 \Delta T = u_1, \tag{2.125}$$

where $a_1, \ldots, a_3$ are constant coefficients representing engine characteristics. The banking actuator comprising aileron servomotor and aircraft rolling motion is described by the following differential equations:

$$\begin{aligned} a_4 \ddot{\sigma} + a_5 \dot{\sigma} &= \delta_A \\ a_6 \ddot{\delta}_A + a_7 \dot{\delta}_A + a_8 \delta_A &= u_2, \end{aligned} \tag{2.126}$$

where $a_4, \ldots, a_8$ are constant coefficients representing aileron servo and aircraft rolling characteristics. The electrical inputs, $u_1(t), u_2(t)$, are supplied by either the pilot or the autopilot according to the desired flight path.

Example 2.2. Automatic control of rotation about the longitudinal axis (roll) is an important example of flight control systems. Several flight applications result in a decoupling of roll from other degrees of freedom (pitch, plunge, forward motion, yaw, and sideslip). While there is a significant aerodynamic interaction among roll, yaw, and sideslip in aircraft, such a coupling does not exist in spacecraft and rockets. Instead, rolling missiles and spinning spacecraft have an inertia coupling between pitch and yaw, as well as between plunge and sideslip. Aerodynamically and inertially coupled dynamics require multivariable control design methods to be considered later. However, there are many situations in which roll can be controlled as a single-axis rotation. Examples include roll-rate regulation of spin stabilized missiles, axisymmetric spacecraft, fighter aircraft, and bank-to-turn missiles.

The simplest roll autopilot is for nonspinning rockets (such as launch vehicles) where an opposing rolling control moment is provided for bringing any roll-rate disturbance to zero. As roll-rate is the coupling between pitch and yaw motions, keeping roll-rate zero uncouples the two transverse rotations, thereby enabling a separate design of pitch and yaw autopilots. Hence, a classical attitude control system can be designed based upon separate roll, pitch, and yaw loops, provided that roll regulator works much faster than either the pitch or the yaw autopilots.

Roll control of rockets that are not required to bank for turning normally consists of a regulator that quickly drives an initial roll-rate to zero. In such cases, roll-rate, $p(t)$, is fed back through a rate gyro (see later) to generate a control rolling moment via control surfaces (fins or exhaust vanes) deflection, $\delta_{\mathrm{f}}(t)$. Consider the following first-order roll-rate dynamics:

$$J_{xx}\dot{p} = L_p p + L_f \delta_{\mathrm{f}}, \tag{2.127}$$

whose unforced response to initial roll-rate disturbance, $p(0)$, is given by:

$$p(t) = p(0)\mathrm{e}^{tL_p/J_{xx}}. \tag{2.128}$$

As the damping in roll ($L_p < 0$) is generally quite small in magnitude for rockets, the roll-rate proportional feedback increases the damping of the overall control system,

$$\delta_{\mathrm{f}} = -Kp, \tag{2.129}$$

where $K > 0$, resulting in the following closed-loop initial response:

$$p(t) = p(0)\mathrm{e}^{t(L_p - KL_f)/J_{xx}}. \tag{2.130}$$

The feedback gain, K, is suitably adjusted in order to achieve a desired settling time, t_{s}, for the roll-rate to settle to within $\pm 2\%$ of the initial disturbance:

$$t_{\mathrm{s}} = -\frac{J_{xx}}{L_p - KL_f}\ln(0.02). \tag{2.131}$$

Generally, the deflection of the control surfaces is limited by aerodynamic effectiveness, $|\delta_{\mathrm{f}}| \leq \delta_{\max}$. In order to ensure that the maximum deflection is not exceeded in normal operation, the regulator gain is selected such that

$$K \leq \frac{\delta_{\max}}{|p(0)|}. \tag{2.132}$$

Of course, such a restriction can be imposed only if an apriori knowledge of expected roll disturbance magnitude, $|p(0)|$, is available by a careful analysis.

2.8 Flight Sensors

Sensors are an integral part of every automatic control system because they supply information about the actual state of the system. In flight applications, sensors are necessary for measuring both translational and rotational motion of the flight vehicle relative to an reference frame approximated to be inertial, as well as that

relative to the atmosphere. Therefore, the flight can be broadly classified as either (a) motion sensors or (b) flow sensors. In motion sensors we have Doppler radars, accelerometers, gyroscopes, horizon, and sun/star scanners, while the flow sensors include airspeed, vertical speed, angle-of-attack, and angle of sideslip sensors.

Virtually all sensors work on the general principle of producing an electrical voltage proportional to the motion variable being measured, and are thus called *voltage transducers*. By calibrating the voltage output, e_y, against the motion variable, y, (i.e., displacement, speed, or acceleration) one can have a linear functional relationship of the following type:

$$e_y(t) = ay(t) + b, \tag{2.133}$$

where a, b are calibration constants. The range of validity of (2.133), $y_a \leq y \leq y_b$ is called the *linear range* of the sensor. Outside the linear range, sensors suffer from nonlinearities like hysteresis, deadzone, and saturation, and therefore cease to be useful. Clearly, a good sensor is the one that has the largest possible linear range.

Being based upon electromagnetism, most flight sensors have at their heart the Faraday's law of induction and are generally of the noncontact type for eliminating noise due to friction. For measuring displacement, *Hall effect* and *linear variable differential transformer* (LVDT) transducers can sense the varying direction of a magnetic field relative to a fixed plate or coil, while angular rate measurement is possible by *incremental encoders* and *back e.m.f* based tachometers. Variations of these basic sensing devices can be found in all flight sensors, such as accelerometers, flow sensors, and rate-integrating gyros that produce displacement of a mass or spring, and rate gyros that produce angular rate outputs. An alternative angular position and rate measurement are provided by the *optical encoders*, which have a rotating transparent disc with some coded opaque areas. A light source and a photo detector "read" the optical pattern resulting from the disc's position at a given instant, which is then translated by a microprocessor to determine the angle and speed of the shaft. As they are based upon digital signals, the optical encoders are less prone to high-frequency noise that plagues analog sensors.

The traditional attitudinal sensors in flight vehicles are gyroscopes that are based upon the torque produced by displacing the axis of a spinning rotor. The study of gyroscopic motion is termed *gyrodynamics* and is our next topic of discussion. Although state-of-the art "gyros" have moved away from rotors and are instead based upon tuning forks, oscillating crystals, and laser "rings" for better ruggedness and fidelity, it is instructive to study the physical characteristics of a classical gyroscope.

2.8.1 Gyrodynamics

Rotors are widely used as both actuators and sensors in flight dynamic plants. They are also present in the form of airbreathing engines in an aircraft, and can affect

its stability and control. Spin stability of an axisymmetric rotor (wheel) – termed gyroscopic stability – is the basic principle behind a gyroscope (in short, gyro), which is a device commonly employed in flight control applications.

A gyroscope consists of a wheel spinning at a constant rate[6] mounted on the flight vehicle in such a way that the wheel's spin axis can pivot in some special directions called *gimbals*. If there is only one gimbal, the wheel can tilt in only one direction and such a gyroscope is called a *single-axis gyro*. If there are two gimbals, the wheel can tilt with respect to the vehicle in two directions and the resulting gyro is termed a *two-degree-of-freedom gyro*. Lastly, there is the *fully gimbaled gyro* consisting of three gimbals, in which the wheel's axis always maintains a fixed direction irrespective of the vehicle's orientation.

When electric motors are used to change the wheel's spin axis relative to the vehicle, the gyroscope acts as an actuator. However, if the gimbals are restrained by springs and viscous dampers, the wheel experiences a torque resulting in gimbal displacements that can be measured by Hall effect/LVDT/optical encoder devices. Thus, a gyro becomes a sensing device for the inertial angular velocity of the flight vehicle and is at the heart of an *inertial measurement unit* (IMU). We will next consider the typical gyroscopic applications in automatic flight control.

2.8.1.1 Rate Gyro

Let us consider a gyroscope that is used to sense a single-axis rotation rate of a flight vehicle. As shown in Fig. 2.14, the single degree-of-freedom rate gyro consists of a rotor spinning relative to a gimbal at a constant angular momentum, H_r, driven by a *servomotor* about the axis *ox*. The gimbal axis, *oy*, can turn by a small angle, $\theta(t)$, relative to the flight vehicle through a restraining mechanism consisting of a linear spring of stiffness, k, and a linear, viscous damper of damping constant, c. The flight vehicle's rotation about the body axis, *oz*, by an inertial angle, ψ, and rate, $\dot{\psi}$, is to be sensed.

As the angular speed of the rotor relative to the gimbal is constant, and the direction of its angular momentum, $\mathbf{H_r}$, does not change relative to the gimbal (due to a rigid construction), there is no change in the rotor's angular momentum relative to the gimbal. Thus, the rate of change of $\mathbf{H_r}$ in the inertial space due to the combined rotation of the vehicle and gimbal is given by:

$$\begin{aligned}\dot{\mathbf{H}}_\mathbf{r} &= \boldsymbol{\omega}_\mathbf{r} \times \mathbf{H}_\mathbf{r} = (\dot{\theta}\mathbf{j} + \dot{\psi}\mathbf{k}) \times H_\mathrm{r}(\cos\theta\mathbf{i} - \sin\theta\mathbf{k}) \\ &= H_\mathrm{r}[-\dot{\theta}(\cos\theta\mathbf{k} + \sin\theta\mathbf{i}) + \dot{\psi}\cos\theta\mathbf{j}]. \end{aligned} \tag{2.134}$$

[6]The wheel's speed is maintained constant by a feedback control system called *servomotor*, which works by taking an angular speed feedback from a tachometer (or an incremental angle encoder) as a sensor, and applies a torque by a direct-current(DC) motor as the actuator.

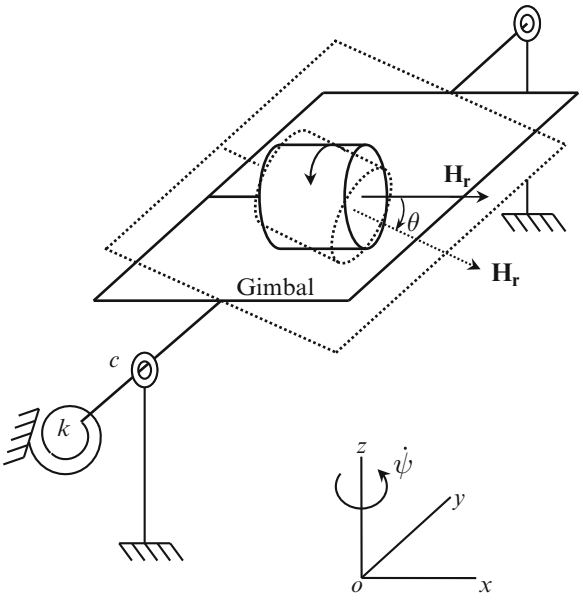

Fig. 2.14 A single degree-of-freedom rate gyroscope

This change of angular momentum results in a torque about the gimbal axis, oy, as well as small transverse torques about ox and oz. While the axial torque causes gimbal rotation, the transverse torques are absorbed by the rotor-gimbal bearing. As both gimbal angle, θ, and gimbal rate, $\dot{\theta}$, are kept small by the restraining spring and damper, we can approximate (2.134) by the linear relationship,

$$\dot{\mathbf{H}}_\mathbf{r} \simeq H_\mathrm{r}\dot{\psi}\mathbf{j}. \tag{2.135}$$

By Newton's second-law, the rate of change of the rotor's angular momentum is equal to the net torque experienced by the rotor, which by Newton's third-law, is equal and opposite to the torque applied by the rotor on the gimbal. Therefore, the gimbal's linearized dynamical equation can be written as follows:

$$J\ddot{\theta}(t) + c\dot{\theta}(t) + k\theta(t) = -H_\mathrm{r}\dot{\psi}(t), \tag{2.136}$$

where J is the moment of inertia of the gimbal and rotor assembly about the axis oy. Equation (2.136) has the following equilibrium solution, $\theta(t) = \theta_\mathrm{e}$, in the steady-state ($t \to \infty$), obtained by letting $\ddot{\theta} = \dot{\theta} = 0$:

$$\theta_\mathrm{e} = -\frac{H_\mathrm{r}\dot{\psi}}{k}, \tag{2.137}$$

which implies a gimbal angle proportional to the vehicle's rotation rate. For this reason, the gyroscope of Fig. 2.14 is called a *rate gyro*, as it can be calibrated to measure a vehicle's rotational rate about the input axis. Two (or more) rate gyros mounted on mutually perpendicular body axis can provide information about a vehicle rotating steadily about multiple body axes. A sudden change in the vehicle's rate, however, will take some time to be registered as the equilibrium gimbal angle output. The time taken to approximately reach the steady-state for a given change in the vehicle's rate depends upon the damping constant, c, as well as the moment of inertia, J, while the equilibrium value of the gimbal angle, (2.137), depends only upon the ratio of the rotor's angular momentum, H_r with the spring stiffness, k. By adjusting this latter ratio, the rate gyro can be made more (or less) sensitive to the vehicle's rate. On the other hand, by adjusting the damping constant, the gyro dynamics can be speeded up, or slowed down, making its respond quickly (or slowly) to change in vehicle's rate.

A voltage transducer (such as Hall effect sensor or LVDT) of constant gain, K_θ, is invariably employed to convert the output angle, $\theta(t)$, into a corresponding voltage, $e_\theta(t) = K_\theta\theta(t)$, which can be easily fed back, or otherwise manipulated by suitable electrical networks according to a specific control law. The transducer gain, K_θ, can be selected based on the desired sensitivity.

Taking the Laplace transform of (2.136) with zero initial conditions ($\theta(0) = \dot{\theta}(0) = 0$ and $\psi(0) = \dot{\psi} = 0$), we have the following *transfer function* (Chap. 3) for the rate gyro, relating the Laplace transforms of the gimbal angle (output), $\Theta(s)$, and the vehicle's inertial rotational rate (input), $s\Psi(s)$:

$$\frac{e_\theta(s)}{s\Psi(s)} = -\frac{K_\theta H_\mathrm{r}}{Js^2 + cs + k}. \tag{2.138}$$

As the rate gyro dynamics is usually much faster than the vehicle's rotation, the transfer function given by (2.138) is practically replaced by the following rate gyro gain constant:

$$K_{rg} = \frac{K_\theta H_\mathrm{r}}{k}. \tag{2.139}$$

2.8.1.2 Rate-Integrating (Displacement) Gyro

If the restraining spring is removed from the rate gyro, the transfer function of the resulting mechanism becomes

$$\frac{\Theta(s)}{s\Psi(s)} = -\frac{H_\mathrm{r}}{s(Js + c)}. \tag{2.140}$$

or,

$$\frac{\Theta(s)}{\Psi(s)} = -\frac{H_\mathrm{r}}{Js + c}. \tag{2.141}$$

It is clear that the resulting gyro is capable of measuring either the vehicle's angular rate, $\dot{\psi}$, through an integral action or its angular displacement, ψ, by a proportional, steady-state, equilibrium gimbal angle, θ_e,

$$\theta_e = -\frac{H_r \psi}{c}. \tag{2.142}$$

Therefore, such a gyro is called a *rate-integrating* gyro (or *displacement gyro*). The rate-integrating gyro can be made more (or less) sensitive to the vehicle's rotation by adjusting the viscous damping constant, c. Additionally, the linear transducer gain, K_θ, is used to adjust the sensitivity of the output voltage, $e_\theta(t)$.

For a gyro with a fast response, the transfer function is replaced by a scaled integral when the rate is input,

$$\frac{\Theta(s)}{s\Psi(s)} = \frac{K_{rig}}{s} = -\frac{K_\theta H_r}{cs}, \tag{2.143}$$

or by a constant gain when the angular displacement is input,

$$\frac{\Theta(s)}{\Psi(s)} = K_{rig} = -\frac{K_\theta H_r}{c}. \tag{2.144}$$

The first-order transfer function of the displacement gyro implies an exponential gimbal angle output for an indicial change in the vehicle's attitude,

$$\theta(t) = -\frac{H_r}{c}\left(1 - e^{-\frac{c}{J}t}\right). \tag{2.145}$$

The time-lag with which the gyro can track a changing vehicle attitude is thus given by the time-constant, $T = \frac{J}{c}$. By increasing c, the speed of response is increased, but the sensitivity is reduced. Hence, a balance must be struck between the speed and the sensitivity of a displacement gyro.

The integral action provided by the rate-integrating gyro is a valuable feature in reducing the steady-state error in a closed-loop system, and enables PID controller implementation (Chap. 3). A combination of rate and rate integrating gyros can handle most practical attitude control tasks.

Example 2.3. Consider a rate gyro with the following characteristics: $H_r = 10^4$ g cm^2/s, $J = 34$ g cm^2, $k = 3.03 \times 10^5$ g cm^2/s^2, and $c = 5{,}000$ g cm^2/s. The gimbal angle response is converted into electrical voltage, e_θ, by a linear voltage transducer with a constant gain 100 V/rad.

(a) Evaluate the gimbal angle response for the rate gyro to a step change (Chap. 3) in the vehicle's angular rate by 0.1 rad/s.
(b) By removing the spring, i.e., making $k = 0$ the rate gyro is converted into a rate-integrating gyro. The transducer gain for the rate-integrating gyro is reduced to 10 V/rad. Find the response of the rate-integrating gyro to a step change in the vehicle's angular orientation by 0.1 rad.

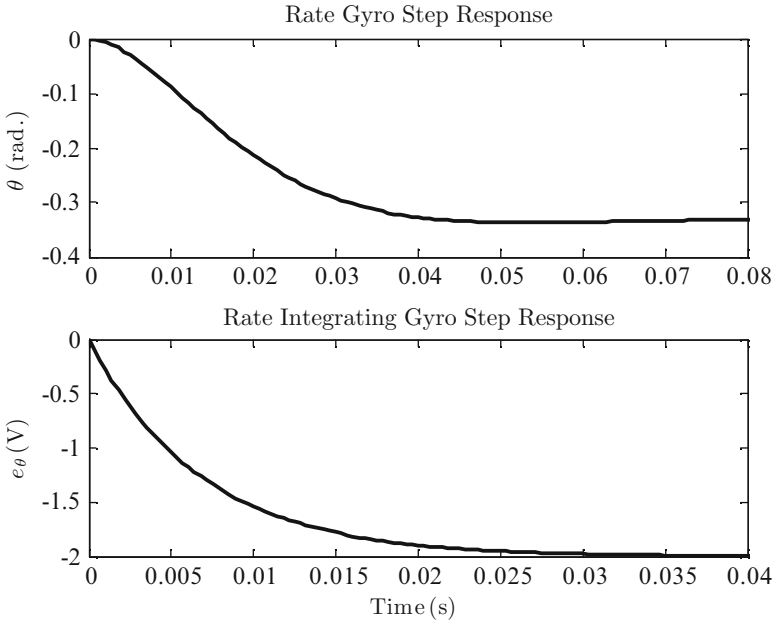

Fig. 2.15 Individual responses of rate and rate-integrating gyros to a step change in the vehicle's angular orientation by 0.1 rad

The necessary computations are carried out using the MATLAB-CST commands *tf* and *step* as follows:

```
>> num=[0 -10000];den=[34 5000 3.03e5];sys=tf(num,den);[y1,t1]=step(sys);
>> num=[0 -10000];den=[34 5000];sys=tf(num,den);[y2,t2]=step(sys);
```

The two step responses are compared in Fig. 2.15. Note that the rate-integrating gyro has a settling-time of 0.04 s that is about half that of the rate gyro. Application of a gyro is restricted to sensing vehicle dynamics about ten times slower than the settling-time of the gyro.

A common single-axis gyro is the *directional gyro* for measuring a vehicle's yaw angle (heading angle) and thus the direction of flight in the horizontal plane. Of course, the directional gyro can measure the heading accurately only if the angular displacements of the vehicle about the other two axes (roll and pitch) are small.

2.8.1.3 Two-Degree-of-Freedom Gyroscope

Consider a wheel mounted on a case through a bi-axial mechanism called *inner gimbal* and *outer gimbal* – as shown in Fig. 2.16 – that allows a bi-directional variation of the wheel's spin axis relative to the case. Such a gyro is termed a two-degree-of-freedom gyroscope. The case, in turn, is rigidly attached to a flight

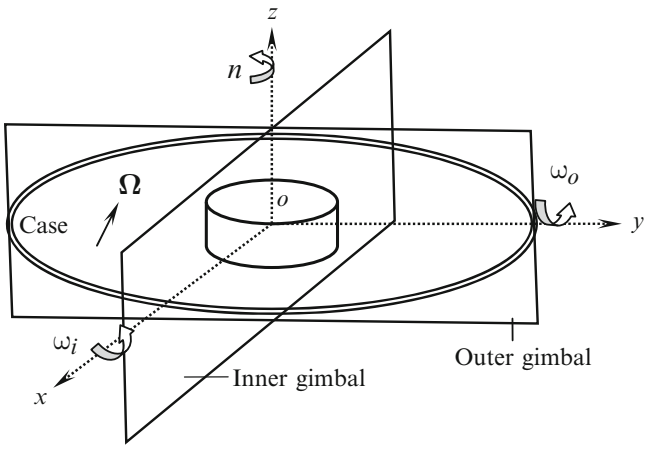

Fig. 2.16 The two-degree-of-freedom gyroscope

vehicle that is rotating with an angular velocity, $\boldsymbol{\Omega}$, with respect to an inertial frame of reference. The wheel is spinning at a rate, n, relative to the inner gimbal about the axis of symmetry, oz, as shown in Fig. 2.16. As the gimbals are always parallel to the wheel's transverse axes, ox, and oy, respectively, we call the wheel-fixed principal body frame $(\mathbf{i}, \mathbf{j}, \mathbf{k})$ the *gimbal axes*. The angular velocity of the inner gimbal with respect to the outer gimbal is $\omega_{\mathrm{i}}\mathbf{i}$, and $\omega_{\mathrm{o}}\mathbf{j}$ is that of the outer gimbal relative to the case (vehicle).

The wheel's inertial angular velocity can be expressed as follows:

$$\boldsymbol{\omega} = n\mathbf{k} + \omega_{\mathrm{i}}\mathbf{i} + \omega_{\mathrm{o}}\mathbf{j} + \boldsymbol{\Omega}, \tag{2.146}$$

while the net angular momentum of the wheel is the following:

$$\mathbf{h} = nJ_{zz}\mathbf{k} + J_{xx}(\omega_{\mathrm{i}}\mathbf{i} + \omega_{\mathrm{o}}\mathbf{j}) + \mathsf{J}\boldsymbol{\Omega}, \tag{2.147}$$

where

$$\mathsf{J} = \begin{pmatrix} J_{xx} & 0 & 0 \\ 0 & J_{xx} & 0 \\ 0 & 0 & J_{zz} \end{pmatrix}, \tag{2.148}$$

and

$$\boldsymbol{\Omega} = \Omega_x\mathbf{i} + \Omega_y\mathbf{j} + \Omega_z\mathbf{k} \tag{2.149}$$

is the flight vehicle's angular velocity resolved in the gimbal axes. The following torque is experienced by the wheel due to its changing angular momentum (2.8):

$$\begin{aligned} \mathbf{M}^{\mathrm{w}} &= M^{\mathrm{w}}{}_x\mathbf{i} + M^{\mathrm{w}}{}_y\mathbf{j} + M^{\mathrm{w}}{}_z\mathbf{k} \\ &= \frac{\mathrm{d}\mathbf{h}}{\mathrm{d}t} = \dot{\mathbf{h}} + \boldsymbol{\omega} \times \mathbf{h}, \end{aligned} \tag{2.150}$$

where

$$\dot{\mathbf{h}} = J_{xx}\left[\left(\dot{\Omega}_x + \dot{\omega}_i\right)\mathbf{i} + \left(\dot{\Omega}_y + \dot{\omega}_o\mathbf{j}\right)\right] + J_{zz}\left(\dot{\Omega}_z\right)\mathbf{k}. \tag{2.151}$$

On taking the cross product and collecting terms in (2.150), we have

$$M^{\mathrm{w}}{}_x = J_{xx}\left(\dot{\Omega}_x + \dot{\omega}_i\right) + \left(J_{zz} - J_{xx}\right)\left(\Omega_y\Omega_z + n\Omega_y + \omega_{\mathrm{o}}\Omega_z + n\omega_{\mathrm{o}}\right) \tag{2.152}$$

$$M^{\mathrm{w}}{}_y = J_{xx}\left(\dot{\Omega}_y + \dot{\omega}_o\right) + \left(J_{xx} - J_{zz}\right)\left(\Omega_x\Omega_z + n\Omega_x + \omega_{\mathrm{i}}\Omega_z + n\omega_{\mathrm{i}}\right) \tag{2.153}$$

$$M^{\mathrm{w}}{}_z = J_{zz}\dot{\Omega}_z. \tag{2.154}$$

If the vehicle is spinning at a constant angular velocity that is small in comparison with the wheel's, one can approximate the torque experienced by the wheel as follows:

$$M^{\mathrm{w}}{}_x \simeq \left(J_{zz} - J_{xx}\right)\left(n\Omega_y + n\omega_{\mathrm{o}}\right) \tag{2.155}$$

$$M^{\mathrm{w}}{}_y \simeq \left(J_{xx} - J_{zz}\right)\left(n\Omega_x + n\omega_{\mathrm{i}}\right) \tag{2.156}$$

$$M^{\mathrm{w}}{}_z \simeq 0. \tag{2.157}$$

By having springs and dampers at the two gimbal locations, the torque components $M^{\mathrm{w}}{}_x, M^{\mathrm{w}}{}_y$, and gimbal rates, $\omega_{\mathrm{i}}, \omega_{\mathrm{o}}$, can be made to produce respective angular displacements, that can be measured and calibrated in a manner similar to the single-axis rate gyro. Thus, the vehicle's spin rates, Ω_x, Ω_y, are obtained from (2.134) and (2.135). However, the third angular velocity component, Ω_z, along the wheel axis cannot be measured. By removing the gimbal restraining springs, the vehicle's angular displacements (rather than the rates) can be measured in a manner similar to the rate-integrating gyro.

A *vertical gyro* is a special two-degree of freedom gyro mounted in such a way that its spin axis is always vertical. Consequently, it can measure pitch and roll angular displacements (or rates) of the vehicle (but not yaw). Such a gyro is also called an *artificial horizon* in aircraft flight displays and provides a basic reference for maintaining a wings-level (unbanked), horizontal attitude. The *Sperry* autopilot of 1909 was based on a vertical gyro, and was tasked principally with maintaining a wings-level attitude during cruise of the early aircraft. Its utility was demonstrated in the long-distance flights by many aviation pioneers, often in bad weather, or at night (such as the solo, transatlantic flight undertaken by Lindbergh in 1927).

The vertical gyro output voltages can be amplified, and used to directly drive electric motors on mutually perpendicular axes, for either moving the control surfaces or tilting a rocket nozzle for thrust deflection. Therefore, a vertical gyro can perform the important role of a two-axis attitude controller. Examples of the first such gyroscopic flight control systems were the unmanned *V-1* "flying bomb" and the *V-2* rocket of the 1930s and 40s, and have continued to be useful in the present age in the form of *inertial navigation systems* for airliners, unmanned aircraft, long-range missiles, and spacecraft.

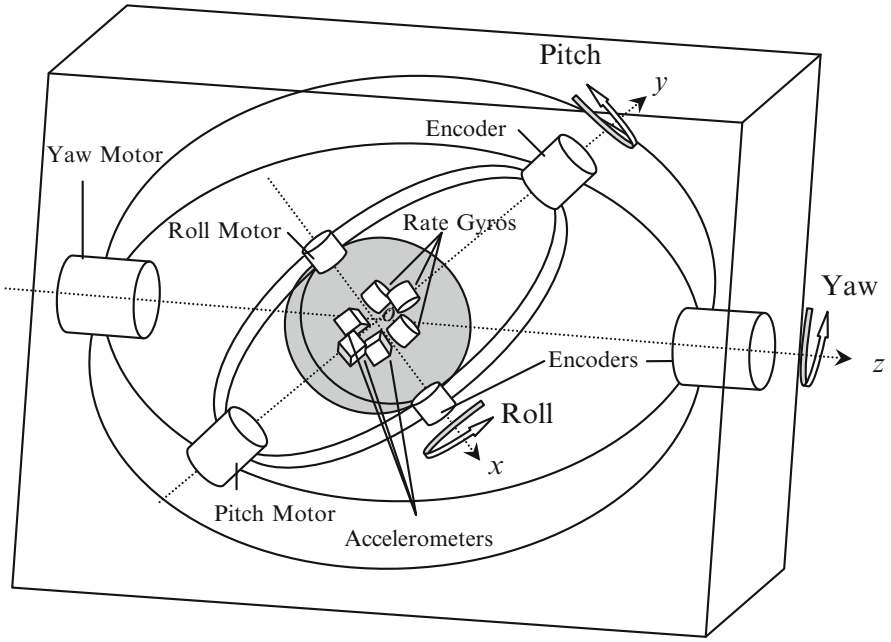

Fig. 2.17 Fully gimbaled, gyro stabilized platform of an inertial measurement unit (IMU)

2.8.2 Inertial Measurement Units

Inertial measurement units (IMU) are a set of gyros and accelerometers that produce motion variables as outputs. Traditionally, the IMU consists of a fully gimbaled gyro platform on which the motion sensors are mounted. It contains three gimbal axes, the inner gimbal, *ox*, the middle gimbal, *oy*, and the outer gimbal, *oz*, which are typically aligned with the vehicle's roll, pitch, and yaw axes, as shown in Fig. 2.17. Each gimbal is driven by a servomotor for keeping the gyro platform fixed in inertial space eventhough the vehicle may have simultaneous rotations about all principal axes. The angle encoders mounted on the gimbal axes provide a feedback to the servos. Such a platform is said to be three-axis stabilized, much like a spacecraft (Chap. 7). The accelerometers and rate gyros mounted on the platform generate the angular rates and displacements by integration [3]. The angular displacements can also be obtained from the gimbal axes encoders by measuring the roll, pitch, and yaw inclinations of the vehicle relative to the platform.

For initially erecting the platform to a desired orientation, distant star constellations are employed as an inertial reference. Conversely, by measuring the angular deviation of the vehicle from the fixed platform, the vehicle's spatial coordinates at any given time relative to distant stars can be computed. This forms the basis of the typical *inertial navigation system* (INS) that is found in virtually every long-range flight vehicle. In order to work in a curved flight path around the Earth, the INS

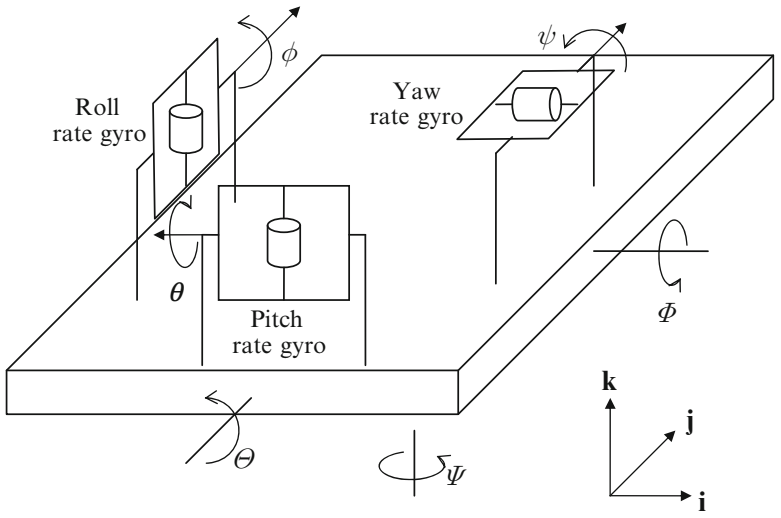

Fig. 2.18 A gyro stabilized platform with three rate gyros

must have a platform that is not exactly stationary, but continuously tilts itself as the vehicle moves, in order to maintain a nearly horizontal reference attitude. Thus, the gimbal servos driving the platform must track the rate, $\dot{\theta} = v/(R_0 + h)$, where R_0 is the planet's radius, v the speed, and h the constant altitude of the vehicle. Interestingly, the required angular acceleration of the platform can be obtained from the linear acceleration, a, sensed by an accelerometer according to $\ddot{\theta} = a/(R_0 + h)$, which is the equation of motion of a simple pendulum of length $R_0 + h$. Such a pendulum is called *Schuler's pendulum* and thus the required adjustment of the platform is known as Schuler's tuning.

Example 2.4. Consider a three-axis, gyro stabilized platform consisting of three identical rate gyros mounted about the roll, pitch, and yaw axes as shown in Fig. 2.18. The angular rate sensed by each gyro is fed to a servomotor, which applies a corrective, restoring torque to the platform. Let Φ, Θ, Ψ be the platform's roll, pitch, and yaw displacements, respectively, relative to an inertial frame. The roll rate gyro senses the relative angular rate, $\dot{\Phi}$, and undergoes an inertial gimbal displacement, ϕ, about the pitch axis according to the rate gyro transfer function,

$$\frac{\phi(s)}{s\Phi(s)} = -\frac{H}{Js^2 + cs + k} = G(s), \tag{2.158}$$

where H is the constant angular momentum of the rotor, and J, c, k the moment of inertia, viscous damping coefficient, and spring stiffness, respectively, about the gimbal axis. The net gimbal rotation relative to the platform is given by:

$$\alpha = \phi - \Theta, \tag{2.159}$$

which yields an electrical voltage output signal, $e_\alpha = K\alpha(s)$, via a transducer of gain K. Similarly, the gimbal rotations of the pitch and yaw rate gyros relative to the platform are

$$\begin{aligned} \beta &= \theta + \Phi \\ \sigma &= \psi - \Theta, \end{aligned} \tag{2.160}$$

respectively, with the identical transfer function given by:

$$\frac{\theta(s)}{s\Theta(s)} = \frac{\psi(s)}{s\Psi(s)} = G(s), \tag{2.161}$$

and the respective voltage pick-offs, $e_\beta = K\beta$ and $e_\sigma = K\sigma$. Since the restoring servomotor torques, τ_x, τ_y, τ_z, are directly proportional to the driving voltages, $e_\alpha, e_\beta, e_\sigma$, respectively, and are related by the same servomotor transfer function, $F(s)$, we write

$$\begin{aligned} \tau_x(s) &= F(s)e_\alpha(s) \\ \tau_y(s) &= F(s)e_\beta(s) \\ \tau_z(s) &= F(s)e_\sigma(s). \end{aligned} \tag{2.162}$$

On substituting (2.158)–(2.161), we have the following *transfer matrix* (Chap. 3) relating the control torques to the platform angular deviations:

$$\begin{Bmatrix} \tau_x(s) \\ \tau_y(s) \\ \tau_z(s) \end{Bmatrix} = \begin{bmatrix} sKF(s)G(s) & -KF(s) & 0 \\ KF(s) & sKF(s)G(s) & 0 \\ 0 & -KF(s) & sKF(s)G(s) \end{bmatrix} \begin{Bmatrix} \Phi(s) \\ \Theta(s) \\ \Psi(s) \end{Bmatrix}. \tag{2.163}$$

Such a coupled relationship between input and output variables is termed *multivariable control*. In Chap. 3, we shall consider design of such control systems.

While gyro stabilized platforms have been traditionally employed in most high-performance flight vehicles (airliners, satellite launch vehicles, cruise and ballistic missiles, and satellites), of late they have been replaced by IMU units that are directly strapped on to the vehicle's body frame. Such strapdown IMUs have the advantage of simplicity and ruggedness due to the presence of smaller moving parts compared to the gyro stabilized platform. They are also free from the errors inherent in gyros, such as drift, bias, misaligned rotors, and other nonlinearities. But the question naturally arises: how can a moving platform provide an inertial attitude reference? The simple answer is, it does not need to. The strapdown IMUs have gyros for measuring the angular orientation of the body-fixed axes on which the three accelerometers are mounted, thereby providing the attitude and acceleration of the vehicle relative to a reference state of the vehicle itself, rather than an inertial

reference frame. The attitude and acceleration data is then processed by a computer in order to generate the vehicle's orientation, position, and velocity in space. In other words, the mechanical INS reference provided by the gyro stabilized platform is replaced by a mathematical one. With the availability of the high-speed digital computers, it has become possible to compute the vehicle's attitude and navigational state in real time from the strapdown IMU data. Furthermore, the availability of the global positioning system (GPS) allows in-flight realignment of the strapdown accelerometers' axes, which was impossible with the gyro stabilized IMU.

The traditional gyros and mechanical accelerometers of the past have been replaced by modern solid-state electronic devices that have no moving parts for a better ruggedness and accuracy. An example is the *ring laser gyro* (RLG) that works on the principles of laser optics rather than Newton's laws. Similarly, the mechanical accelerometers have been replaced by piezoelectric sensors that can offer a better resolution and dynamic range of measurement.

2.9 Summary

Flight dynamics consists of motion of the center of mass (translational dynamics) and rotation of the vehicle about the center of mass (attitude dynamics). While translational flight dynamics is referred to an inertial frame, the attitude dynamics describes the rotation of a body-fixed frame relative to a nonrotating coordinate frame. Aircraft flight regards the local horizon frame to be inertial, whereas rocket and space flight is more commonly approximated by treating a planet-fixed frame as an inertial reference frame. The aerodynamic forces and moments depend upon the vehicle's attitude relative to the velocity vector, which is resolved in the wind axes system. The stability axes, having one axis along the equilibrium flight direction, are useful in carrying out the small perturbation approximation for aircraft dynamics plant. The dependence of aerodynamic forces and moments on the shape, size, speed, and orientation of the vehicle as well as the atmospheric properties is modeled by the angle-of-attack, the angle of sideslip, and nondimensional flow parameters – Mach number, Reynolds number, Knudsen number. Flight sensors are important as the eyes and ears of the automatic controller, and consist of motion sensors and flow sensors. A gyroscope is a typical motion sensor that can be employed in measuring either single- or multiaxis rotations. A single-axis rate gyro produces an electrical output proportional to the angular rate, while a rate-integrating gyro indicates the net angular motion from a reference point. A vertical gyro is a two degree-of-freedom sensor with roll and pitch capability. A fully gimbaled gyro platform is the classical heart of the inertial measurement unit (IMU) employed in inertial navigation systems (INS), while the strapdown IMU can be found in the modern INS and is normally coupled with the global positioning system (GPS) for a better accuracy and ruggedness. A generic flight dynamics plant is driven by both control and environmental inputs, and can be linearized about a nominal trajectory.

Exercises

2.1. Derive the kinematic equations of motion for the 3-2-1 Euler angle sequence, $(\psi)_3, (\theta)_2, (\phi)_1$, in terms of the body rates, (P, Q, R). Identify the singular points of this attitude representation.

2.2. A spacecraft is in an elliptical orbit around the Earth ($\mu = 398600.4$ km^3/s^2, mean radius, $R_0 = 6378.14$ km) with an eccentricity of 0.2 and a semimajor axis of 15,000 km. Determine the radius, speed, and flight path angle when the true anomaly is 60°.

2.3. A spacecraft has its perigee (minimum radius) point given by speed of 8 km/s and altitude 300 km above the Earth's surface. Calculate the position, velocity, and time since perigee when the true anomaly is 100°.

2.4. For the spacecraft of Exercise 2.3, what are the celestial position and velocity coordinates at the true anomaly of 100° if the orbital plane is given by $\Omega = 30°$, $i = 60°$, and $\omega = 200°$?

2.5. Using the coordinate transformation between the celestial and the local horizon frames, derive the relationship among orbital inclination, velocity azimuth, and latitude of a spacecraft.

2.6. An axisymmetric spacecraft with principal moments of inertia, (J_x, J_x, J_z) (products of inertia zeros), is initially in a nonrotating state. It has a small rotor with moment of inertia about the spin axis, J_r, spinning about the spacecraft's axis of symmetry at a rate, ω_r. Determine the final spacecraft angular velocity if: (a) the rotor axis is turned by a 45° angle about spacecraft's body axis, $\mathbf{k}$, and (b) the rotor is speeded-up to twice the original rate.

2.7. Derive the equations of motion relative to the body-fixed principal axes for the flight of a rocket in a vertical plane ($\psi = \text{const.}$). Assume a constant thrust, T, with mass variation given by

$$\dot{m} = -\frac{T}{v_\mathrm{e}},$$

where v_e is the constant exhaust speed of the propellant gases. The thrust vector's inclination in the principal body-fixed frame is given by the angles μ_1, μ_2, as shown in Fig. 2.10. The drag force is given by:

$$\mathcal{D} = \frac{1}{2}\rho v^2 S C_\mathrm{D},$$

where ρ is local atmospheric density, S a reference area, and C_D the drag-coefficient. The rocket must have a zero force normal to the flight path as well as a zero rolling moment. Use $(\psi)_3, (\theta)_1, (\phi)_3$ for the rocket's principal body-axis orientation relative to the local horizon frame. Qualitatively discuss how an automatic controller should maintain flight in the vertical plane despite lateral atmospheric disturbances due to planetary rotation and winds.

2.8. Derive the equations of motion relative to the body-fixed principal axes for the flight of an airplane in a horizontal plane ($\phi = 0$). Assume a constant engine thrust, T, the drag force is given by the same expression as in Exercise 2.7, and normal force and sideforce are given by:

$$Z = -\frac{1}{2}\rho v^2 S C_{\mathrm{L}}(\alpha),$$

$$Y = \frac{1}{2}\rho v^2 S C_Y(\beta),$$

where ρ is local atmospheric density, S a reference area, and C_{L}, C_Y are nondimensional coefficients. Use the Euler angles, $(\psi)_3, (\theta)_2, (\phi)_1$, for the airplane's principal body-axis orientation relative to the local horizon frame. Qualitatively discuss how an automatic controller should maintain flight in the horizontal plane despite lateral atmospheric disturbances due to planetary rotation and winds.

2.9. Can a rate gyro respond to either an impulsive or a step change in a vehicle's angular displacement? Answer this question using the final-value theorem of Laplace transform. Simulate the gimbal output response of the rate gyro of Example 2.3 to the following inputs:

(a) An impulsive angular displacement of the vehicle by 0.1 rad.
(b) A step change in the vehicle's angular orientation by 0.1 rad.

2.10. Consider attitude control of a thrust vectoring rocket (Exercise 2.7) in space, where the aerodynamic torque is negligible. The rocket is axisymmetric with $J_{yy} = J_{zz}$ and has an angular velocity perturbation, $\boldsymbol{\omega} = Q\mathbf{j} + R\mathbf{k}$, with respect to the equilibrium attitude. The control system is based upon two-degree-of-freedom gyro outputs, pitch rate, Q, and yaw rate, R, for driving the thrust gimbal angles, ϵ, μ, according to the following control laws:

$$\epsilon = -k_1 R; \qquad \mu = -k_2 Q,$$

where k_1, k_2 are positive constants called *feedback gains* and are related to the voltage amplifiers between the gyro outputs and the gimbal motor inputs.

(a) Derive the equations of rotational kinetics of the system.
(b) Analyze the stability of the control system.
(c) Derive an expression for the closed-loop response of the system when $k_1 = k_2 = k$, subject to the initial condition, $Q(0) = Q_0, R(0) = R_0$.

2.11. From the flight model of Example 2.1, derive the linearized plant for level flight of an aircraft relative to a spherical, rotating Earth with airspeed, $v(t)$, azimuth, $\psi(t)$, latitude, $\delta(t)$, and longitude, $\lambda(t)$, as the state variables. Control inputs are the electrical signals, $u_1(t)$ and $u_2(t)$ to the engine and aileron actuators, respectively. Wind speed, $v_{\mathrm{w}}(t)$, and wind azimuth, $\psi_{\mathrm{w}}(t)$, are stochastic (random) inputs, regarded as disturbances (process noise). Assume that a constant altitude is

maintained by a separate control system – not modeled here – called *altitude hold autopilot*, which ensures that the vertical component of the lift balances the weight at all times.

2.12. For the gyro stabilized platform of Example 2.4, derive the transfer matrix relating the servomotor torques and the platform's angular deviations if $H = 3 \times 10^{-3}$ N.m.s, $J = 10^{-5}$ kg m^2, $k = 0.1$ N.m/rad, $c = 1.5 \times 10^{-3}$ N.m.s/rad, $K = 100$ V/rad. The servomotor transfer function is given by:

$$F(s) = \frac{10^4}{s^2 + 200s + 10^4} \text{ N.m/V}.$$